Application of Computer-based Methods to Guide the Development of Novel Sirtuin Inhibitors

Dissertation

zur Erlangen des akademischen Grades

Doctor rerum naturalium

(Dr. rer. nat.)

vorgelegt der Naturwissenschaftlichen Fakultät I - Biowissenschaften -

der Martin-Luther-Universität Halle-Wittenberg

von

M.Sc. Berin Karaman

geboren am 15. April 1986

Gutachter/in:

1. Prof. Wolfgang Sippl, Halle

2. Prof. Mike Schutkowski, Halle

3. Prof. Gerhard Ecker, Vienna

Datum der Disputation: 02 November 2015

Abstract

Sirtuins are promising therapeutic targets which have been linked to the pathogenesis of several diseases including metabolic disorders, viral and parasitic diseases, neurodegeneration and cancer. During the last decade much effort has been devoted to discover novel sirtuin modulators with drug like properties. However, most of these compounds showed limited potency and subtype selectivity. Moreover, structural information is not available for most of them.

In the current work, as a first step, we addressed the issue of structure-based optimization of sirtuin inhibitors. We demonstrated that protein-inhibitor complexes of sirtuin isoforms can be obtained by means of ligand docking and applying a short molecular dynamics (MD) simulation. This method is faster and less complex than such applications and can be also applied to other protein targets beside sirtuins. We determined a significant correlation between the binding free energy of the compounds estimated by MM-GBSA calculations and *in vitro* data. The developed MM-GBSA protocol is computationally inexpensive and can be applied as a post-docking filter in virtual screening campaigns to identify novel sirtuin inhibitors.

Next, we established the structural basis of Sirt2-selective inhibition with the identification of a new potent drug-like inhibitor; SirReal2. X-ray crystal structures of Sirt2 in complex with SirReal2 revealed a ligand-induced rearrangement of the active site and formation of a yet-unexploited allosteric binding pocket. In order to rationalize the SirReal2-mediated high-isotype selectivity, sequence and structural alignments were performed within the members of sirtuin family. Assuming that SirReal2 binds into the other sirtuin subtypes in a similar fashion, we generated homology models and carried out docking studies of SirReal2. The obtained results demonstrate that the residues that form the SirReal2 binding pocket differ significantly within the sirtuin family and minor sequence variations hamper the correct orientation of SirReal2.

Moreover, we developed photoswitchable sirtuin inhibitors by merging the structure of photochromic diarylmaleimides with the pharmacophore of a known sirtuin inhibitor. The new compounds exhibited potent Sirt2-selective inhibition with regard to the Sirt1 and Sirt3 isoforms. Docking studies could explain the structure activity/selectivity relationship observed for these compounds.

Addditionally, human Sirt2 inhibitors has been shown to posses strong effects on both the life span and reproduction of *Schistosoma mansoni*, the main pathogen of schistomiasis. Thus, we

expanded our interests into smSirt2 as a new antiparasite target. Upon screening of an in-house library, we identified a number of potent novel smSirt2 inhibitors. Due to the absence of the smSirt2 crystal structure, we first generated a homology model (HM) for this enzyme. We could rationalize the binding interactions of the detected inhibitors with smSirt2-HM by means of docking.

In order to decipher the complex nature of sirtuins in cancer, potent and isoform selective sirtuin inhibitors are highly in need. In this context, we established docking- and pharmacophore-based virtual screening methods. The potential of these methods were verified using the newly developed African natural product anticancer database (AfroCancer) and already known anticancer drug targets.

Keywords: epigenetics, sirtuin, Schistosoma mansoni, cancer, docking, homology modeling, MM-GBSA, virtual screening.

Kurzfassung

Sirtuine sind vielversprechende therapeutische Targets, die mit der Pathogenese von verschiedenen Erkrankungen, einschließlich Stoffwechselstörungen, virale und parasitäre Erkrankungen, Neurodegeneration und Krebs verbunden sind. Während des letzten Jahrzehnts wurde viel Aufwand gewidmet, um neue Sirtuin-Modulatoren mit wirkstoffähnlichen Eigenschaften zu entdecken. Jedoch zeigten die meisten dieser Verbindungen begrenzte Affinität und Subtypselektivität. Darüber hinaus sind für die meisten dieser Verbindungen keine strukturellen Informationen verfügbar.

In der vorgelegten Arbeit haben wir uns mit der strukturbasierten Optimierung von Sirtuin-Inhibitoren beschäftigt. Wir zeigten, dass Inhibitoren von den verschiedenen Sirtiun-Isoformen mittels Ligandendocking und Anwendung einer kurzen Moleküldynamik (MD) Simulation erhalten werden können. Dieses Verfahren ist schnell und wenig aufwendig und kann auch auf andere Protein-targets neben Sirtuine angewendet werden. Eine signifikante Korrelation zwischen den mittels MM-GBSA geschätzten freien Bindungsenergien und den in *vitro Daten* der Verbindungen wurde festgestellt. Das entwickelte MM-GBSA Protokoll kann effizient durchgeführt und als Postdocking-Filter im virtuellen Screening zur Identifikation neuer Sirtuin-Inhibitoren angewendet werden.

Als nächstes haben wir die strukturelle Basis für die selektive Hemmung von Sirt2 durch die Identifizierung eines neuen potenten wirkstoffähnlichen Inhibitor, nämlich SirReal2, aufgeklärt. Die Röntgenkristallstrukturen von Sirt2 im Komplex mit SirReal2 zeigten eine liganden-induzierte Umlagerung der aktiven Bindungstasche und die Bildung einer allosterischen Bindungstasche. Um die SirReal2 Isotypselektivität zu erklären, wurden Sequenz- und Strukturalinierung von allen Mitgliedern der Sirtuin-Familie durchgeführt. Unter der Annahme, dass SirReal2 in die anderen Sirtuin-Subtypen in einer ähnlichen Weise bindet, entwickelten wir Homologiemodelle und führten Docking-Studien für SirReal2 in diesen Modellen durch. Die erhaltenen Ergebnisse zeigten, dass die Aminosäurereste, die die Bindungstasche von SirReal2 bilden, sich unter den verschiedenen Sirtuine deutlich unterscheiden und dass geringfügige Unterschiede in der Sequenz die korrekte Orientierung von SirReal2 in der Bindungstasche behindern.

Außerdem entwickelten wir photo-schaltbare Sirtuin-Inhibitoren durch die Zusammenlegung der Struktur der photochromen Diarylmaleimide mit dem Pharmakophor eines bekannten Sirtuin-

Inhibitors. Die neuen Verbindungen zeigten eine hohe Sirt2 Hemmung und eine Selektivität über Sirt1 und Sirt3 Isoformen. Docking-Studien könnten die für diese Verbindungen beobachten Struktur Aktivität bzw. Selektivität Beziehung erklären.

Des Weitern wurde gezeigt, dass Inhibitoren der humanen Sirt2 eine starke Auswirkungen auf sowohl die Lebensdauer als auch die Reproduktion von Schistosoma mansoni, der wichtigste Erreger von Schistosomiasis, besitzen. So haben wir unsere Interessen auf smSirt2 als neues antiparasitäre Target erweitert. Beim Screening von einer hauseigenen Datenbank identifizierten wir einige potent;e neue smSirt2 Inhibitoren. Aufgrund der Abwesenheit der smSirt2 Krystallstruktur, wurde zuerst ein Homologiemodell (HM) für dieses Enzym generiert. Wir könnten die Bindungsinteraktionen der ermittelten Inhibitoren mit smSirt2 -HM durch Docking rationalisieren.

Um die komplexe Rolle von Sirtuine in Krebserkrankungen zu entschlüsseln, sind potente und isoformselektive Sirtuin-Inhibitoren stark benötigt. In diesem Zusammenhang haben wir Docking- und Pharmakophor-basierte virtuelles Screening-Methoden etabliert. Das Potenzial dieser Methoden wurde mit dem neu entwickelten „African natural product anticancer database (AfroCancer)“ und bereits bekannten Targets für die Krebstherapie überprüft.

Schlagwörter: Epigenetik, Sirtuine, Schistosoma mansoni, Krebs, Docking,

Homologiemodellierung, MM-GBSA, virtuelles Screening.

Acknowledgments

The present work has been one of the most memorable journey and the greatest challenge in my academic life which started when I came to Halle (Saale) in early spring of 2011. Fulfilling it would not have been possible without the support, patience and guidance of a number of people along the way whom I owe a big thank.

I would like to thank, first and foremost, my supervisor; Prof. Dr. Wolfgang Sippl. My deepest gratitude goes to him for giving me the chance to join his research group and for his endless support and guidance to overcome the humps during the course of this work. He has inspired me deeply as an academician and played a role model as an advisor – who is enthusiastic and perfectionist about his research, who always finds time for his students to comment and assist on countless pages of reports, manuscripts, thesis and etc., and above all who is kind and thoughtful like a parent to his students.

I wish to thank our collaborators at the University of Freiburg, Prof. Manfred Jung and his research team, who contributed immensely in different stages of this work by carrying out various biochemical experiments. Here, my special thanks go to Tobias Rumpf for conducting X-ray crystallographic studies and numerous in vitro tests on sirtuins and Matthias Schiedel for synthesizing and testing sirtuin activities of many compounds.

I would also like to take this opportunity to thank all my teachers who assisted me to come this far throughout my educational career and allow me to reach this accomplishment.

My sincere thanks go to all the former and previous members of Research Group Medicinal Chemistry in Institute of Pharmacy in Martin-Luther-University Halle-Wittenberg. I have been very fortunate to work in a friendly and stimulating working environment throughout these past four years. I am very thankful for all the intellectual discussions we had, for all the help that I received and for all the joyful Christmas parties, summer trips, exciting defense celebrations and delicious birthday cakes that we shared together. I was lucky to be a part of an international working community, to get to know many nice and inspiring people and to learn different cultures and cuisines.

I would especially like to thank Dr. Dina Robaa who has been a dear friend, a great colleague and a precious sister to me for the last four years. I am very grateful to her for helping me out and for being a shoulder that I can lean on in all sorts of problems that I have faced both in personal and professional life during my stay in Halle. I enjoyed very much sharing many teas

and coffees together, our long chats, dinners and walks through Peissnitz Park after the school. Thank you for always being with me through all the good times and the bad.

I would also like to express my deepest love and gratitude towards my family. I don't have the words to thank my parents enough for their eternal love since I was born, their endless support and patience over the years and most importantly for giving me the best siblings I could ask for. Being a member of 3K has been the most meaningful privilege of my life which I wouldn't change it for the world. Thank you for always being there for me.

Last but not least, I would like to extend my sincere appreciation to all the friends that I met during my PhD in Germany, and especially to Chris who has become a big part of this journey and my life for the last two years. Thank you for being supportive, understanding and encouraging when things seemed to be so complicated. Thank you for always being there and for caring enough to bear me in my tribulations, through my joy and sorrow.

Dedication

I dedicate this dissertation to my beloved parents Tulin and Bekir Karaman, and my dearest siblings Fatma Nur Karaman Kabadurmus and Ahmet Karaman.

Table of Contents

List of Figures

List of Abbreviations

3D: three dimensional

ACS2: acetyl-CoA-synthetase 2

AD: applicability domain

ADMET: absorption, distribution, metabolism, excretion and toxicity

BFE: binding free energy

BLAST: basic local alignment search tool

clogP: calculated logP

CoMFA: comparative molecular field analysis

CPS1: carbamoyl phosphate synthetase I

CR: calorie restriction

DOPE: discrete optimized protein energy

DMP: dimethylpyrimidine

DNP: dictionary of natural products

EC: extended C-pocket

EMBLEBI: european molecular biology laboratory-european bioinformatics institute

FEP: free energy perturbation

FOXO1: forkhead box O1

HAT: histone acetyl transferase

HDAC: histone deacetylase

HM: homology model

HTS: high-throughput screening

ITC: isothermal titration calorimetry

LBVS: ligand-based virtual screening

LIE: linear interaction energy

logP(o/w): logarithm of the octanol/water partition coefficient

LOO: leave one out

MD: molecular dynamics

MM-GBSA: molecular mechanics-generalized born surface area

MM-PBSA: molecular mechanics poisson-boltzman surface area

MM-PB(GB)SA: molecular mechanics/poisson-boltzmann (generalized born) surface area

MOE: molecular operating environment system

MEFs: mouse embryonic fibroblasts

MW: molecular weight

NCA: nicotinamide

NPACT: naturally occurring plant-based anticancer compound-activity-target

NRot: number of rotatable bonds

OAADPr: O-acetyl-ADP-ribose

PCA: principal component analysis

PDB: protein data bank

PEPCK1: phosphoenolpyruvate carboxykinase

PGC-1α: PPARγ coactivator 1 alpha

PME: particle mesh ewald

PPARγ: peroxisome proliferator-activated receptor gamma

PSA: polar molecular surface area

QSAR: quantitative structure-activity relationship

RMSD: root mean square deviation

SAR: structure activity relationships

SASA: solvent-accessible surface area

SBVS: structure-based virtual screening

SirReal: sirtuin rearranging ligand

Sirt: sirtuin

SREBP1c: sterol regulatory element-binding protein 1c

STAC: sirtuin activating compound

TI: thermodynamic integration

UniProt: universal protein resource

vdW: van der Waals

VS: virtual screening

WHO: world health organization

…
Two roads diverged in a wood, and I—
I took the one less traveled by,
And that has made all the difference.

Robert Frost

1. Introduction

1.1. Epigenetics: Re-programing Genetics

The term epigenetics can be defined literally as "around the genetics" which involves the heritable alterations in gene expression that are not encoded in the underlying DNA sequence itself [1]. Considering the fact that human cells contain the same exact human genome sequence but they do not evolve in the same manner in the process of cell differentiation and formation of neurons, muscles, and organs implies that there is a control mechanism which operates 'around the genome', hence the term granted for describing this process, epigenome.

To date, three different mechanisms have been shown to be involved in epigenetic regulation including 1) DNA methylation, 2) post-translational modifications of histones and 3) non-coding RNA-mediated gene silencing [2]. Misregulation of these epigenetic processes can lead to aberrant activation or silencing of genes. In 1983, Feinberg and Vogelstein presented for the first time the connection between epigenetic alterations and cancer [3]. In their study, the authors showed that patients with colon and lung cancers had significant DNA hypomethylation in the affected tissues in comparison to the adjacent normal tissues. Furthermore, many enzymes have been discovered to be involved in epigenetic regulation through chemical modifications of histones and non-histone proteins. Today, the regulation of such epigenetic targets with small molecules has found implications in a wide range of diseases including cancer, metabolic and neurological disorders, inflammation, and parasitic and viral diseases. However, such attempts to make this connection are most often hampered by the lack of potency or selectivity of the compounds of interest or by the complexity of the mechanisms involved.

It is apparent that understanding the relationship between epigenetic processes, deciphering potential epigenetic targets and their roles in physiological pathways, and mapping the translation of genotype to phenotype via the epigenome, have great potential for drug discovery and development for human diseases.

1.2. Histones and DNA Organization in Nucleus

Nucleosomes are the fundamental repeating units of chromatin, which consist of two superhelical turns of DNA wrapped around a histone octamer core (**Figure 1.1.**). The histone

octamer core is formed by two copies of histone proteins H3, H4, H2A and H2B. These nucleosome particles hold in place by the linker histone H1 and form the chromatin subunit known as chromatosome. Chromatosomes are connected to each other with linker DNA and packed by non-histone proteins into a more condensed structure called chromatin [4].

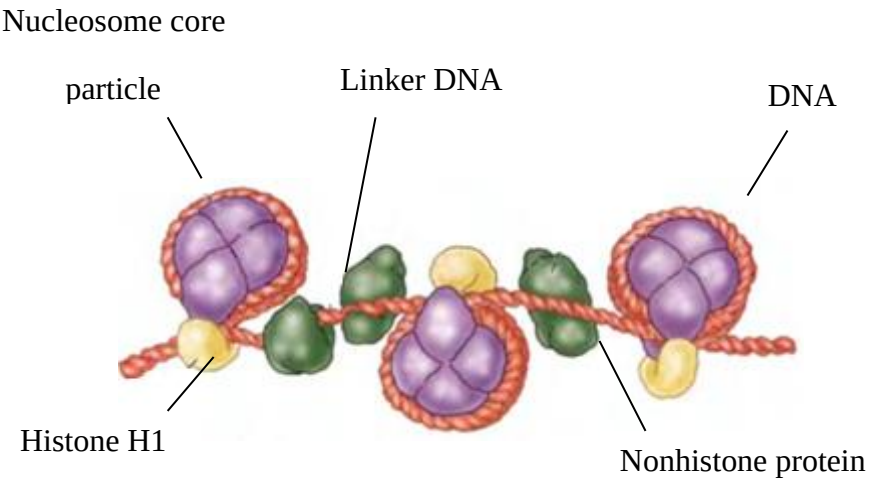

Figure 1.1. Chromatin structure. The DNA is wrapped around nucleosome core particles, namely the histones, and packed by linker histone H1. Linker DNA and nonhistone proteins complement the packaging of human genome in chromatin. Adapted from [4].

This formation allows the approximately two meter long DNA to fit into the cell nucleus. The core histones, which contain high proportion of basic amino acids: arginine and lysine, facilitate binding to the negatively charged DNA. Histones are mainly comprised of a globular histone fold domains, which interacts with other histones and with the DNA in the nucleosome through charged N-terminal tails that extend outside the nucleosome. Histones are modified by covalent post translational modifications of the histone tail such as acetylation, phosphorylation, methylation, and ubiquitinilation and reverse reactions of those modifications. Combination of such modifications, described in literature most often as histone code, allows the regulation of the interactions between the DNA sequence and the histones in an indirect way without changing the genetic information [5]. Thus, the histone code provides an external control mechanism for re-programming the genetic information passed onto the cells.

1.3 Histone Deacetylases (HDACs)

Among the histone modifications, acetylation status of the core histone tails is dependent on the

opposing activities of histone acetyl transferases (HATs) and histone deacetylases (HDACs). HATs acetylate ε-groups of specific lysine residues of histone tails as well as non-histone proteins. On the other hand, HDACs are responsible for the removal of the acetyl group from these residues [6]. While acetylated histones are often associated with transcriptional activation and the increase in gene expression, deacetylated histones are linked to transcriptional repression and gene silencing [7]. Numerous studies have shown that regulation of HDACs activity bears a significant therapeutic value in the treatment of cancer, neurological disorders, and inflammatory diseases (reviewed in [8-12])

To date, 18 HDACs have been identified in humans that can be classified into four groups based on their homology to yeast histone deacetylases: Class I HDACs (HDACs 1, 2, 3 and 8), Class II HDACs (HDACs 4, 5, 6, 7, 9 and 10), Class III HDACs (Sirtuins): Sirtuin -1, -2, -3, -4, -5, -6 and -7) and the recently identified Class IV HDACs (HDACs 11). Class I, II and IV HDACs are more commonly referred to as classical HDACs and depend upon Zn^{+2} ion for the catalytic reactions [6,7]. Class III HDACs are named after their yeast homologue silent information regulator two proteins (Sir2) as sirtuins. Unlike classical HDACs, sirtuins are NAD^{+} dependent for their catalytic mechanisms [13].

1.4. Class III HDACs: Sirtuins

1.4.1. Overall Structure of Sirtuins

Sirtuins have been found in a wide variety of life forms ranging from prokaryotes to eukaryotes. All sirtuins share a conserved catalytic core of ~ 275 amino acids and N- and C- terminal extensions that are variable in length, sequence and secondary structure [14]. The core domain consists of a large Rossman fold domain and a smaller structurally more diverse zinc-binding domain that are connected through four loops in order to form the active cleft (**Figure 1.2.**).

The cofactor binding loop constitutes the most dynamic region in sirtuins which under goes distinct conformational changes dependent on the presence, identity, and binding region of molecules [15,16]. X-ray structures of sirtuins confirmed that the acetyllysine containing peptide substrate and the cofactor NAD^{+} bind to the active cleft from opposite sides of the enzyme.

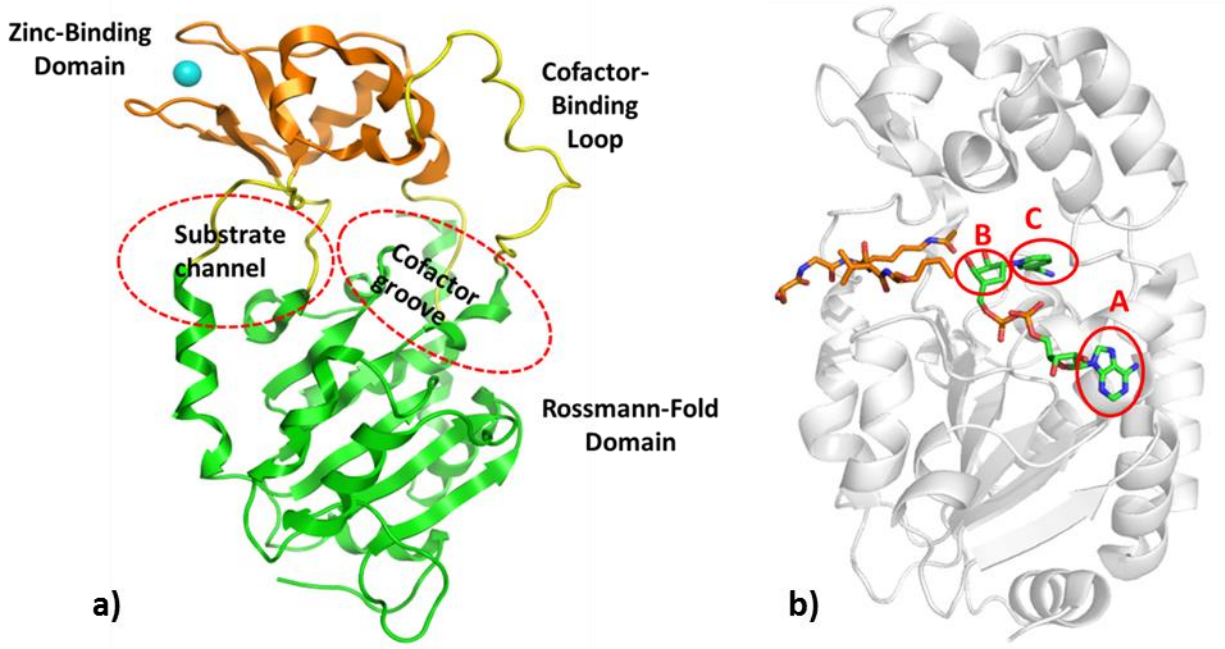

Figure 1.2. Overall structure of sirtuins. **a)** Sirt2 (PDB ID; 1J8F) as an example. The structure of Sirt2 is shown as a cartoon model. The zinc-binding domain and Rossman-fold domain are colored in orange and green, respectively. The four loops (including the cofactor binding loop) that connect the subdomains are colored in yellow. Substrate and cofactor binding pockets are indicated with red circle dashed lines. The zinc ion is shown as a cyan sphere. **b)** Sirt3 (PDB ID; 4FVT) as an example. The structure of Sirt3 is shown as white cartoon model. Sirt3 is bound to the acetylated substrate, ACS2 (acetylCoA synthetase 2) peptide (orange sticks), and carba-NAD (green sticks). The NAD^+ binding region is divided into sites A-C. The A, B, and C sites are indicated by red circles.

Comprehensive kinetic studies and emerging structural data on sirtuins suggested that the acetyllysine binds prior to NAD^+ and induces a significant reorientation of the zinc binding domain relative to the Rossmann fold domain [17,18]. A subsequent rearrangement of conserved residues in the acetyllysine channel results in the correct positioning of the acetylated substrate and binding of NAD^+ in the 'productive conformation' [19]. The NAD^+ binding pocket can be divided into three regions: site A, the adenine binding site; site B, the nicotinamide-ribose binding site and site C, nicotinamide moiety or the free nicotinamide binding site [15]. Site B and C are involved in the catalytic mechanisms regulated by sirtuins.

1.4.2. NAD^+ Dependent Catalytic Mechanism of Sirtuins

Although, NAD^+ dependent deacetylation is the most well-known reaction catalysed by sirtuins, ADP-ribosyl transfer to proteins, NAD^+ hydrolysis, and reformation of NAD^+ through

nicotinamide base-exchange reaction, have also been reported [13]. Furthermore, recent studies have shown that sirtuins can efficiently remove butyryl, crotonyl, octanoyl, malonyl, succinyl, myristoyl, palmitoyl, and other groups from the lysine residue [20-23]. In 2013, Feldman et al. [24] demonstrated that all human sirtuins except Sirt7 (no quantifiable product was observed with Sirt7) are capable of long-chain deacylation activity; however, catalytic efficiencies and substrate preferences were different among the sirtuin isoforms. A recent study showed that NAD^+ levels may affect the catalytic activity of sirtuins and their substrate preferences [25]. Moreover, kinetic analysis revealed that sirtuins display varying degrees of sensitivity to nicotinamide inhibition depending on the acyl substrate.

The catalytic mechanism of sirtuins involves: 1) hydrolysis of NAD^+ to acyl-ADP-ribose and nicotinamide which is followed by 2) acyl group transfer from the peptide substrate to ADPR and 3) formation of deacetylated peptide and a mixture of 2'- and 3'-O-acetyl-ADP-ribose (**Figure 1.3.**).

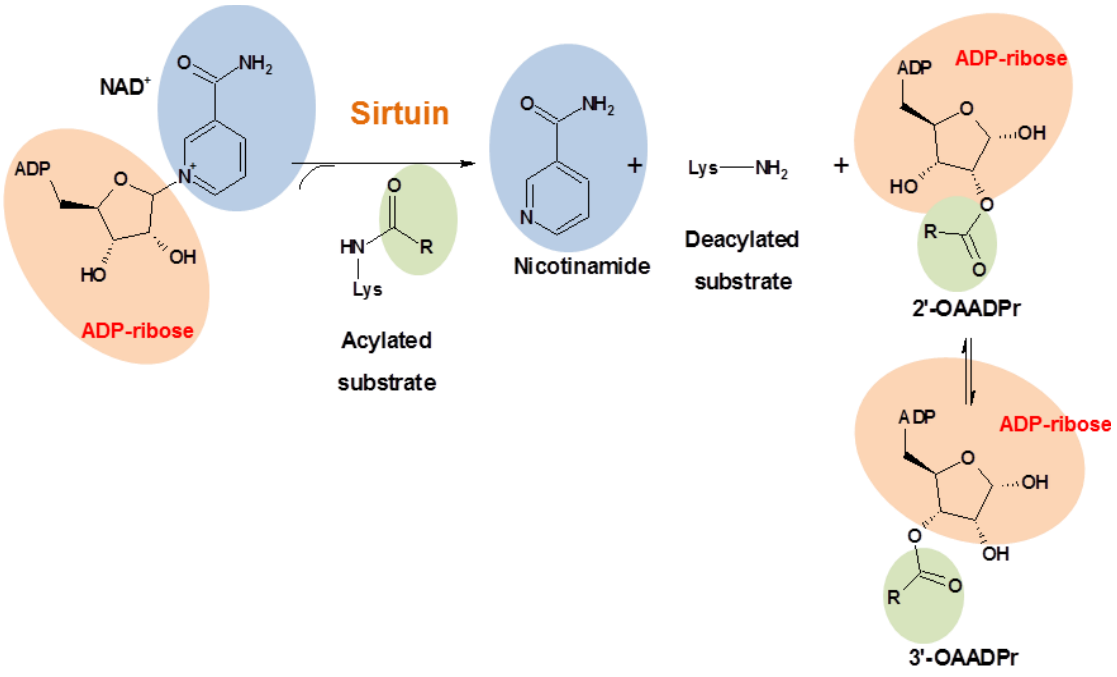

Figure 1.3. Sirtuin-catalyzed protein deacylation and reaction products.

1.4.3. Sirtuins: Subcellular Localization

The identification of Sir2 gene as a regulator of life span has spurred great interest in the studies of mammalian sirtuins since the late 1990s. Until today seven sirtuin isoforms have been

identified in humans; Sirt1-7. Sirtuins are located in different subcellular compartments, including the nucleus (Sirt1, Sirt6 and Sirt7), the cytosol (Sirt2), and mitochondria (Sirt3-5). In addition, recent studies showed that Sirt1 and Sirt2 can shuttle between the nucleus and the cytoplasm and Sirt3 may translocate from the mitochondria to the nucleus as well. Sirt1 possesses both nuclear localization and nuclear export signal regions which were suggested to govern its ability to shuttle between the nucleus and the cytosol. Although, Sirt2 is predominantly localized in the cytoplasm, it also obtains nuclear export signal sequences and shuttles to the nucleus during mitosis. Meanwhile, Sirt3 contains an N-terminal mitochondrial localization sequence which is attributed to its localization in mitochondria [26]. However, Scher et al. [27] demonstrated that full-length Sirt3 localizes in the nucleus under normal cell growth conditions and translocates from the mitochondria to the nucleus under cellular stress. The distinct and dynamic subcellular localization of sirtuin isoforms contributes to their highly divergent substrate preferences and interacting partners. Thus, they have diverse biological functions in cellular processes.

1.4.4. Sirtuins: Disease Relevance

AGING

Among all seven human sirtuins, Sirt1 has been the most extensively studied mammalian sirtuin. Sirt1 deacetylates numerous lysine residues residing at different regions of histones including H1 (K26), H3 (K9, K14) and H4 (16) [28]. The early discovery that Sir2 gene regulates the cell survival and longevity in calorie restriction (CR) [29] coupled with the fact that there is a link between the age-correlated hyperacetylation of H4K16 and accompanying Sirt1 reduction [30], has intensified the investigations of elucidating the role of sirtuins in aging. Recently, Li et al. [31] showed that compared to the wild-type mice, Sirt1-null mice have a shorter life span on both normal and CR diets. Moreover, Sirt1-activating compounds, including resveratrol and other natural polyphenols, and small molecule activators of Sirt1 that are structurally unrelated to resveratrol such as SRT1460, SRT1720, and SRT2183 (**Figure 1.4.**), have been shown to exert similar effects to those of CR, thereby extending life-span and improving metabolic homeostasis [32-35]. These findings have spurred great interest in sirtuins and their regulatory roles in age-related diseases such as metabolic disorders, neurodegenerative diseases and cancer.

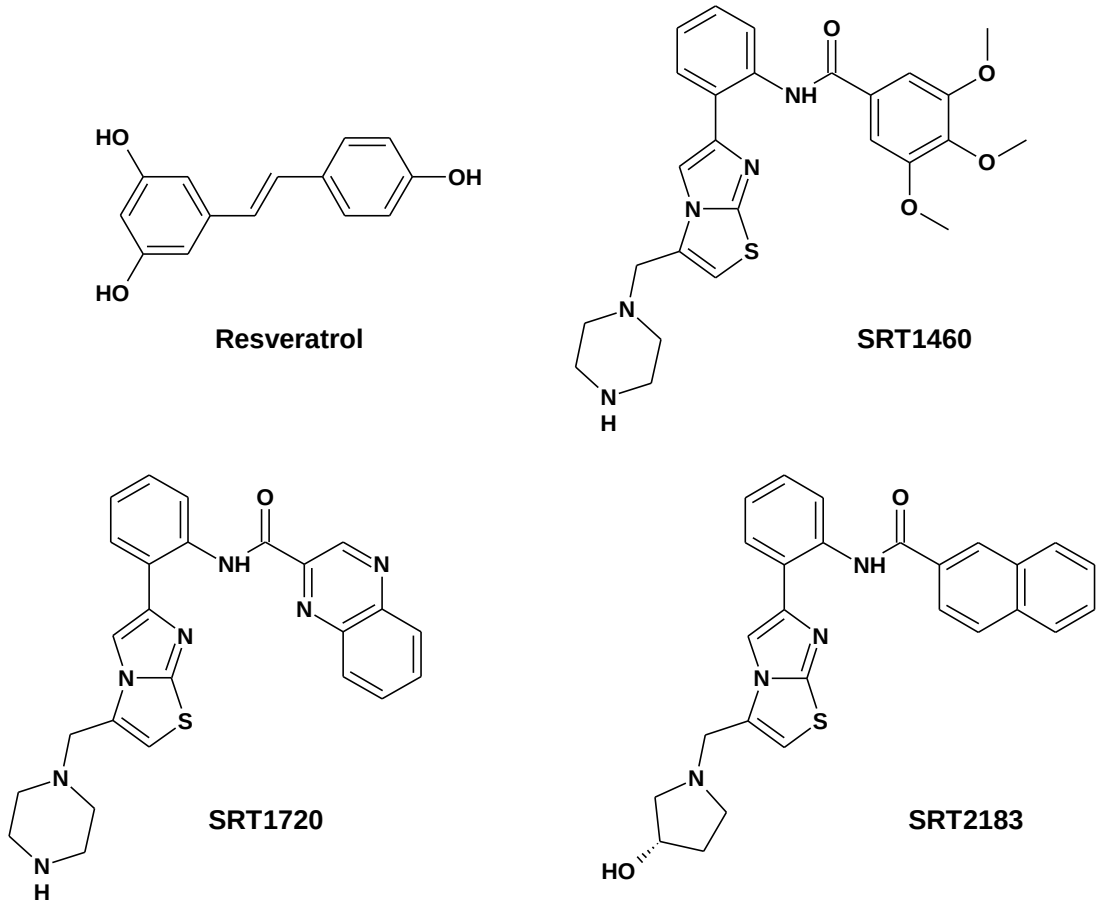

Figure 1.4. Molecular structures of Sirt1-activating compounds.

METABOLIC DISEASES

Sirt1 regulates the metabolic homeostasis via deacetylating a number of non-histone proteins such as peroxisome proliferator-activated receptor gamma (PPARγ), PPARγ coactivator 1 alpha (PGC-1α), sterol regulatory element-binding protein 1c (SREBP1c), and the forkhead box O1 (FOXO1), which results in induction of gluconeogenesis [36], enhancement of insulin sensitivity, fatty acid oxidation [35-37], and repression of lipid synthesis [38].

In addition to Sirt1, Sirt2 is also involved in metabolism. Sirt2 deacetylates and stabilizes one of the key regulator of gluconeogenesis; phosphoenolpyruvate carboxykinase (PEPCK1). Indeed, knocking down Sirt2 resulted in lower blood glucose levels in mice models [39].

Not surprisingly, mitochondrial sirtuins, Sirt3-5, are the main pioneers of energetic adaptation. Sirt3 deacetylates and activates several metabolic substrates associated with fatty acid oxidation, amino acid catabolism, and urea cycle [40-42]. These results indicate that Sirt3 promotes energy

production from alternative energy sources, ketone bodies, and amino acids, under low energy conditions. Unlike Sirt3, Sirt4 represses GDH activity by ADP-ribosylation and reverses the effects of CR [43]. Moreover, Sirt4 was shown to regulate fatty acid oxidation and insulin secretion via the regulation of Sirt1 expression [44] and interacting with insulin degrading enzyme and the ADP/ATP carrier proteins, ANT2 and ANT3 [45], respectively. On the other hand, Sirt5 helps the clearing of ammonia by deacetylating and hence stimulates the carbamoyl phosphate synthetase 1 (CPS1) activity [46].

In sum, these findings suggest that Sirt1-5 work in harmony to mediate the metabolic responses during fasting and cellular stress, regulate glucose, and play a role in lipid homeostasis. Therefore, sirtuins are promising therapeutic targets for metabolic disorders such as diabetes, obesity, and hypercholesterolemia.

CANCER

Since the identification of tumor suppressor p53 as a substrate of Sirt1, there has been a growing interest in elucidating the role of sirtuins in carcinogenesis. Initially, Sirt1 was considered as an oncogene because of its role in repressing the expression and activity of several tumor suppressor and DNA-repair genes (reviewed in reference [47] and [48]). Moreover, Sirt1 expression is upregulated in many cancer types, including colon, prostate and breast cancers and leukemia, supporting that Sirt1 might be oncogenic [49-52].

Recently, it was reported that combination of a novel Sirt1 inhibitor, Ex-527 (**Figure 1.5.**), with an HDAC inhibitor, valproic acid or butyrate, induces apoptosis in human leukemia cells [53]. In addition, Sirt1 promotes apoptosis [54] and suppresses tumor formation [55-57]. Wang et al. [58] demonstrated that Sirt1 plays an important role in genomic stability via regulating histone modifications and DNA repair. Sirt1-null embryo models exhibited altered chromosome morphology, impaired DNA damage response, and reduced DNA damage repair. Furthermore, authors showed reduced Sirt1 levels in various cancer tissues, including bladder, prostate and ovarian cancers, implying that Sirt1 might be a tumor suppressor.

Besides Sirt1, the role of Sirt2 in cancer cell proliferation has also been hotly debated. Increased tumor formation in Sirt2 deficient mice models and down regulation of Sirt2 in glioma, gastric carcinoma, and non-small lung cancer types, suggest a tumor suppressor role for this enzyme [59-61]. On the other hand, pharmacological inhibition of Sirt2 with small molecules has been

useful in treating a wide variety of cancer cell lines (reviewed in [48]), therefore a few examples will be discussed.

Sirtinol (**Figure 1.5.**) was one of the first small molecules discovered as a dual inhibitor of Sirt1/2 with IC_{50} value of 131 µM and 38 µM for Sirt1 and Sirt2, respectively [62]. Sirtinol was reported to inhibit tumor growth in oral, breast, lung, and prostate cancers [63-66]. Another dual inhibitor of Sirt1 (IC_{50} = 56 µM) and Sirt2 (IC_{50} = 59 µM), cambinol (**Figure 1.5.**), inhibited tumor growth in Burkitt lymphoma xenografts [67]. Moreover, Zhang et al. [68] discovered a sirtuin inhibitor, AC-93253 (**Figure 1.5.**), with selective inhibitory activity against Sirt2 (IC_{50} = 6.0 µM) over Sirt1 (IC_{50} = 45.3 µM) and Sirt3 (IC_{50} = 24.6 µM), respectively. Ac-93253 showed cytotoxic effect in prostate, pancreas, and lung cancer cell lines. Collectively, these data retrieved from small molecule inhibitors of Sirt1/2 strengthen the idea that they should be classified as an oncogene.

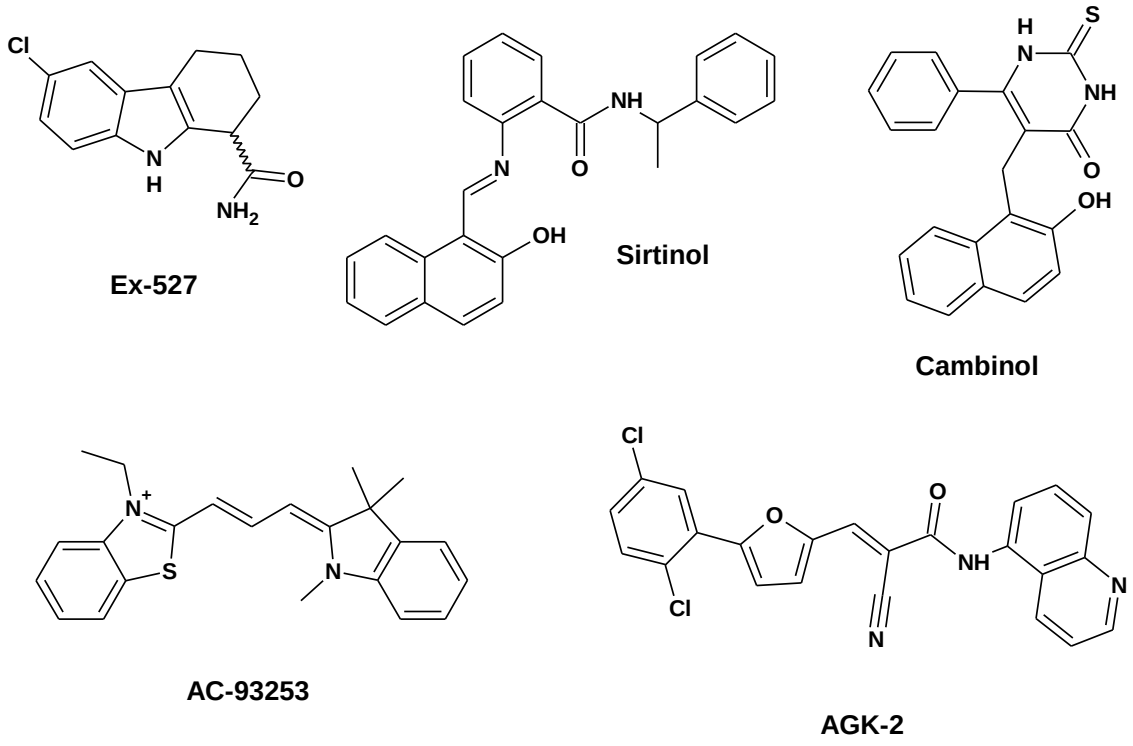

Figure 1.5. Molecular structures of Sirt1and Sirt2 inhibitors.

As for other sirtuins, Sirt3-7, less information is available for their role in cancer biology. Existing data suggests that Sirt3 acts as a tumor suppressor. Kim et al. [69] demonstrated that

Sirt3 knockout mouse embryonic fibroblasts (MEFs) exhibit enhanced superoxide levels, mitochondrial damage and genomic instability. Moreover, Sirt3 deficient MEFs when infected with an oncogene, RAS or MYC, became immortalized. The authors also showed a decreased level of Sirt3 expression in many cancer types including breast, testicular, prostate, head and neck cancers.

Recently, it has been discovered that mammalian target of rapamycin complex 1 (mTORC1) induces cell proliferation via repressing Sirt4 expression and inhibiting GDH activity [70]. It is also shown that Sirt4 is downregulated in several cancer types and appears to modulate tumor cell metabolism. Meanwhile, Sirt6 is suggested to regulate cancer metabolism through repressing aerobic glycolysis and is thus postulated as a tumor suppressor [71]. Indeed, Sirt6 deficient MEFs displayed elevated glucose uptake and tumor formation.

Sirt7 is the least studied human sirtuin whose biochemical mechanism, substrate proteins and physiological functions have not been clarified. Available evidence suggests that inhibition or downregulation of Sirt7 can be beneficial for treating cancer. Ford et al. [72] demonstrated that Sirt7 activates RNA polymerase I (Pol I) transcription and regulates cellular rRNA synthesis. Knockdown of Sirt7 in a human osteosarcoma cell line (U2OS) blocks cell proliferation and triggers apoptosis, suggesting that Sirt7 is crucial for cell viability. Recently, Barber et al. [73] also demonstrated that Sirt7 acts as a tumor promoter through deacetylation of H3K18 and that Sirt7-depletion impairs tumor formation in cancer cell lines including HT1080 (a fibrosarcoma cell line), U2OS and U251 (a glioma cell line).

Taken together, these data illustrate the complex regulatory role of sirtuins in cell proliferation and viability. It is still unclear how sirtuins can display both tumor promoting and tumor suppressing effects and how these play out under different circumstances. Sirtuin tissue-specific knockout mouse models and isoform specific sirtuin modulators would increase our understanding of the mechanism behind carcinogenesis and how sirtuins are involved with this mechanism.

NEURODEGENERATION

Sirtuin functions are also involved in neurodegenerative diseases such as Wallerian degeneration (WD), Alzheimer's disease (AD) and Parkinson's disease (PD). The neuroprotective role of Sirt1 was first shown by Araki et al. in 2004 [74]. In their study, the authors proposed that enhanced NAD^+ levels due to the increased activity of nicotinamide mononucleotide adenylyltransferase1

(Nmnat1) and the subsequent Sirt1 activation was neuroprotective against WD, which occurs upon a nerve cut/crush and results in degeneration of axons. The same year, Brunet et al. [75] demonstrated that Sirt1 can protect cerebellar granule neurons from FOXO-3 mediated cell death. Moreover, Sirt1 was protective against neurodegeneration in transgenic mouse models with p25/Cyclin-dependent kinase 5 (CDK-5) [76], which is associated with neuronal death and pathology of AD [77]. Sirt1 was also required for neuroprotection in transgenic mice with a mutant form of superoxide dismutase 1 (SOD1G37R), which has been linked to human amyotrophic lateral sclerosis [76].

On the contrary, Outerio et al. [78] demonstrated that inhibition or knockdown of Sirt2 reduces α-synuclein dependent toxicity in neurons. Consistent with these findings, Sirt2 inhibition by AGK-2 (**Figure 1.5.**), which inhibits Sirt2 with an IC_{50} of 3.5 μM, was neuroprotective in animal models of PD. Similarly, Sirt2 inhibition reduced sterol biosynthesis via the negative regulation of SREBP-2 which resulted in decreased level of mutant huntingtin inclusions that are responsible for neuronal loss and associated with HD [79].

Little is known about the regulatory roles of other sirtuin isoforms, Sirt3-7, in neurons. Pfister et al. [80] studied for the very first time the effects of all human sirtuin isoforms on neuronal viability. The authors showed that Sirt1 has neuroprotective effects on neurons, which is consistent with the previous published data. In addition, overexpression of Sirt2 in cerebellar granule neurons (CGNs) had an apoptotic effects on healthy neurons, which is in line with the studies showing that neuroprotective response is retrieved upon Sirt2 inhibition. Interestingly, while overexpression of Sirt3 and Sirt6 promoted low potassium (LK) and high potassium (HK) induced neuronal death, Sirt4 and Sirt7 showed no effect. On the contrary, increased expression of Sirt5 localized in both the nucleus and cytoplasm protected CGNs from LK-induced apoptosis. However, in HT-22 neuroblastoma cells Sirt5 was localized in mitochondria and promoted cell death. Together, these data suggests that Sirt5 exerts adverse effects on neuron survival depending upon its subcellular localization.

Although the existing data on how sirtuins function in neurodegeneration is still incomplete, the initial evidence suggests opposing effects of sirtuin isoforms on neuronal viability under similar conditions. Furthermore, it is important to identify the counterparts of sirtuins and account for all posttranslational modifications that can directly or indirectly regulate sirtuins' role in

neurophysiology. Unfortunately, we have still very little information on sirtuin neurobiology to draw meaningful conclusions.

In this chapter, a short introduction was provided on Class III HDACs, sirtuins, and their prominence in epigenetics. For more detailed information on sirtuins, the reader should refer to the first publication, entitled "Structure-based design and computational studies of sirtuin inhibitors". This book chapter provides an extensive overview of the already solved sirtuin crystal structure isoform complexes with substrates and modulators. Moreover, a summary of *in silico* studies that resulted from the development of novel sirtuin inhibitors and activators is also provided.

2. Materials and Methods

Designing small molecules with desired biological activity has been a long-time major goal of the drug discovery process. Today, mainly two interdependent approaches exist, which are used for the identification of new lead compounds: 1) high-throughput screening (HTS) and 2) computer-aided drug discovery and development. High-throughput screening is an experimental screening where large compound libraries of diverse synthetic and natural compounds are tested against disease targets to identify small molecule probes that modulate a specific biological pathway. Although HTS has been successful in providing starting points for drug design, this method suffers from low hit rates, poor time and cost efficiency, and lack of information of the biological target. On the contrary, *in silico* drug design approaches start with a known or suggested binding mode of a molecule to its macromolecular target. Lead structures that mimic similar interactions are either designed or retrieved from large compound libraries and the new information is included iteratively in the drug design process until all desired properties are met. Such methods can highly reduce the number of compounds that need to be experimentally tested and thus, maximize the time and cost efficiency in drug development. The following paragraphs describe the *in silico* drug design techniques applied in this work.

2.1. Homology Modeling

Computer-aided drug design consists of two major approaches; structure-based drug design and ligand-based drug design. Structure-based drug design relies on the three dimensional (3D) structural information of the biomolecular target. Numerous structural genomics projects have widened the determination of the 3D protein structures which are stored in a worldwide archive, the Protein Data Bank (PDB) [81]. By June 2015, the PDB contained approximately 100,000 experimental protein structures [82]. Considering the fact that the Universal Protein Resource (UniProt) Database [83] contains 548,586 manually annotated and non-redundant protein sequence entries in the release 2015_06 of 27-May-15 of UniProtKB/Swiss-Prot [84], there remains a huge gap between known protein sequences and available 3D structures.

Homology modeling also known as “Comparative Protein Structure Modeling” aims to fill this gap by predicting a 3D model for a protein of unknown structure (the target) from proteins that share sequence similarity with known structures (templates) [85,86]. In the literature, many

examples for successful homology models that were used for docking and virtual screening studies have already been reported [87]. Current methods consist of the following steps [86]:

a) Fold assignment and template selection: identification of templates can be done by comparing the target sequence with the sequences in large protein databases either by a pairwise sequence-sequence comparison or using a position-specific scoring matrix (implemented in FASTA [88] and basic local alignment search tool (BLAST) [89]), or using 3D template matching methods that rely on comparison of a protein sequence and a protein of known structure.
b) Target-Template Alignment: the correct alignment of the sequences is highly dependent on the sequence identity and it is more beneficial to use multiple templates where sequence identity drops below (30-40 %) (implemented in Clustal X [90]). Superposing these multiple templates before the alignment helps to obtain more accurate alignment by using information from secondary structure elements in proteins where the sequence similarity is low.
c) Model Building: once the target-template is prepared then the model can be built with different methods. One method is to compile rigid bodies for the conserved core region, loops, and side chains from templates to build the model for the target and then apply a subsequent optimization and minimization process, while putting these rigid bodies together [91] (implemented in COMPOSER [92]). Another method is based on calculating the probable positions of the conserved atoms in the target by using the information from the template. A third method which is implemented in MODELLER [93], depends on spatial restraints to assume the corresponding distances and angles of residues using the knowledge obtained from the template structure.
d) Refinement / Validation / Evaluation of the Models: After a model is built, loops and side chains of the residues should be further studied. For estimating the accuracy of the features in 3D models, programs such as PROCHECK [94] can be used to check the bond lengths, bond angles, side-chain ring planarities, chirality and clashes between nonbonded pair atoms.

The following paragraph describes the homology modelling procedure used in this work (**Figure 2.1.**). The sequence for the protein of unknown structure was taken from UniProt database [83] and saved as a FASTA file. A subsequent protein BLAST search [95] was performed to identify

the proteins that share sequence similarity with known structures (templates). Target-template alignment was done by Molecular Operating Environment 2012.10 (MOE) [96] protein alignment tool MOE-Align. Homology models were then generated using the MODELLER program 9v8 [93]. 10 protein conformations were generated. The model showing the most favourable DOPE (Discrete Optimized Protein Energy) assessment score [97] was selected. The stereochemical quality of the models was validated with PROCHECK [94]. Assignment of the correct protonation state and energy minimization of the homology models were carried out in MOE [96].

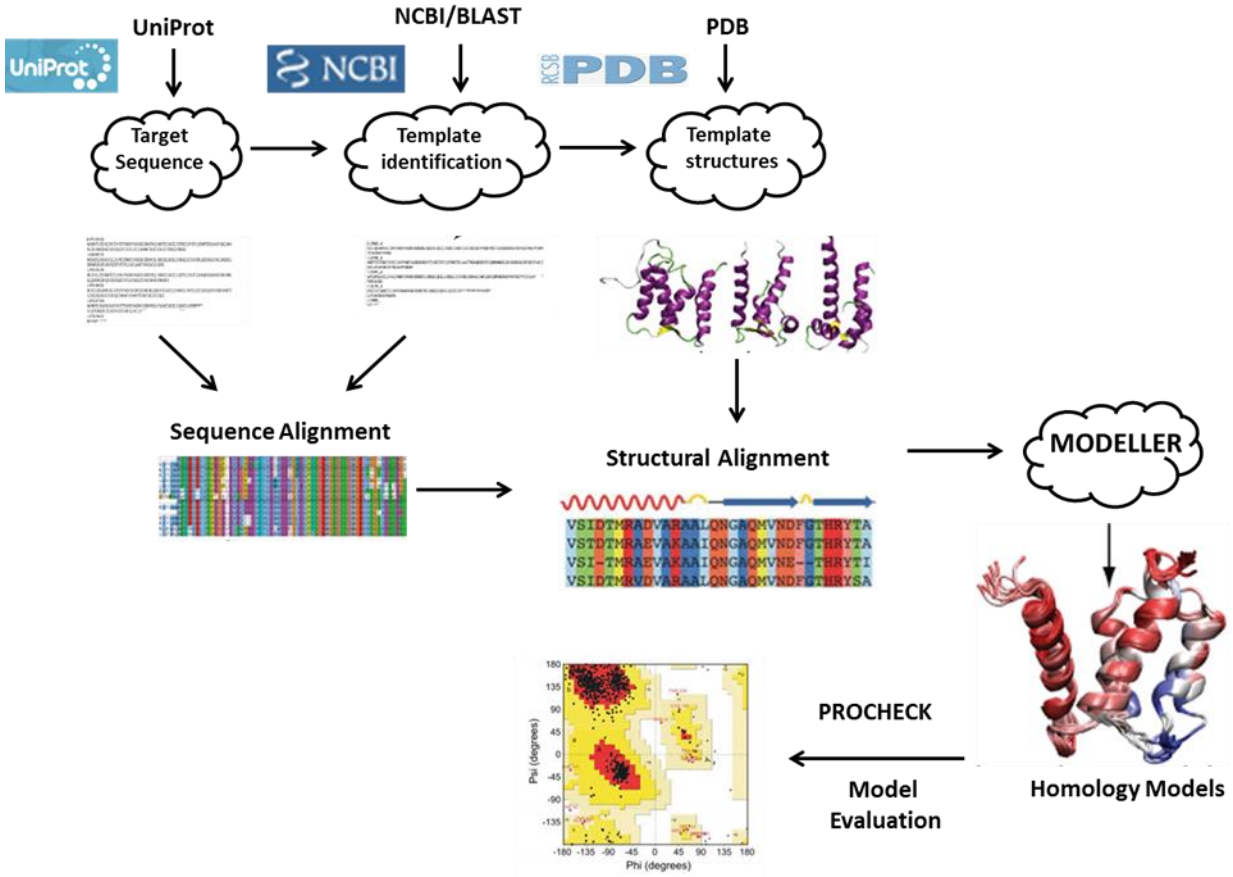

Figure 2.1. Homology modeling workflow used in this work. Adapted from [98] and [99].

2.2. Molecular Docking

Molecular docking can be defined as conformational and orientational sampling of the ligand using the putative binding site of the receptor as a constraint. Once the candidate conformations for the ligand is predicted, their binding affinity must be evaluated, and this is done by means of

a scoring function [100]. Today, molecular docking is the most extensively used and heavily applied structure-based method in drug discovery.

Although docking tools of today are able to model the interactions in the putative binding site and can easily screen large number of molecules, the accurate-assessment of the protein-ligand affinity is still challenging [101]. Considering the balance between the accuracy of calculations and the computational cost, scoring functions were developed on the basis of simplified empirical force fields or potentials of mean force using certain approximations. For example, they usually do not take solvation effects or protein flexibility into account [100,102,103]. Thus, accurate prediction of the binding affinity using docking methodologies remains an elusive goal and there is a need of more precise methods for its evaluation.

As the accuracy of docking / scoring is highly dependent on the ligand and protein preparation, one should address issues such as possible isomers, protonation states of the ligands, and side chain conformations of the protein in the ligand binding site [102]. Ligand preparation could be done manually or by using programs like LigPrep [104] implemented in Schrödinger software.

In addition, the flexibility of proteins is still a big challenge in molecular docking approaches [105]. The most popular methods to overcome this issue are

a) Soft Docking which reduce the van der Waals optimal distances to form more space for the ligand in binding site,
b) The Rotamer-Library Method that use libraries of side chain rotamers,
c) Ensemble Docking where multiple crystal structures are used for the target receptor, or
d) Generating different conformations of the protein via molecular dynamics (MD) simulation [102].

Furthermore, the presence of water molecules can be critical to the binding of the ligand [106]. Unfortunately, while today's docking tools can present or predict the water molecules in the binding site to direct docking, optimization of the water locations upon binding, or presenting the binding free energy contributions of water molecules to the scoring, remains to be dealt with.

In the current work, protein structures were prepared by using the Structure Preparation module in MOE [96]. Protonation states of the structures were determined using the Protonate 3D [107] module in MOE. Protein structures were energy minimized using the AMBER99 force field [108] using a tethering force constant of (3/2) kT/σ2 (σ = 0.5 Å) for all atoms during the minimization. All molecules except the zinc ion were removed from the structures before

docking. Structural bridging of water molecules was included in the binding site of the protein structures before docking whenever it is mentioned.

Docking studies were carried out using the scoring functions within the GOLD 5.2 (Goldscore, Chemscore, ASP and PLP Score) [109-113] and GLIDE (Schrödinger Suite 2012-5.8) (Glide SP and Glide XP scores) [114-117]. The position of the ligands in the crystal structures and homology models was used to define the binding site. Bound water molecules at the binding pocket of the protein structures were considered for docking in the toggle water mode [118] within GOLD docking and were treated as rigid within GLIDE docking. The 20 docking poses were calculated for each ligand. All other options were left at their default values.

2.3. Virtual Screening

2.3.1. Preparation of Compound Libraries

In order to balance the time-cost efficiency, often the chemical space of the search library is decreased with a filter before screening. A simple but straightforward pre-screen approach is to remove the molecules with reactive or undesired functional groups. In the current study, we assessed the toxicological profiles of the virtual libraries by Lhasa's expert knowledge-based predictive tool; Derek software [119]. The Derek system first identifies the chemical substructures within the molecules and then describes the relationship between a particular structural feature and its associated toxic effect [120-123]

In addition, filters that predict the *in vitro* properties of molecules such as ADMET (absorption, distribution, metabolism, excretion and toxicity) properties (reviewed in [124]) are often used to prepare focused libraries. The main aim of ADMET analysis is to eliminate the compounds with undesirable pharmacokinetics in the early stage of drug design and focus exclusively on potential drug candidates with good bioavailability. In order to identify the weak drug candidates in virtual datasets, we calculated a total of 46 ADMET-related properties via the QikProp program [125]. The computed parameters were used to assess the oral absorption, cell permeability, central nervous system penetration abilities, etc. of the compounds.

Moreover, the drug-likeness of the compounds within the search libraries was estimated by Lipinski's rule of five [126]. According to the "rule of five", compounds having more than 5 H-bond donors, 10 H-bond acceptors, a MW greater than 500 Da, and a calculated logP (clogP) greater than 5 are considered to have a poor absorption and permeability. This criterion

contributes to the elimination of compounds with undesirable pharmacokinetic properties and thus, it accelerates the identification of drug-like candidates.

2.3.2. Classification of Virtual Screening Approaches

Virtual screening (VS) is an essential complement of HTS drug discovery process [127]. To identify chemical probes with desired biological activity and to select a limited number of small molecules for experimental testing, various VS methods have been developed in order to screen large compound libraries *in silico*. VS methods of today can be classified into two main groups: ligand-based and structure-based approaches depending on the availability of structural and biological activity data (**Figure 2.2.**).

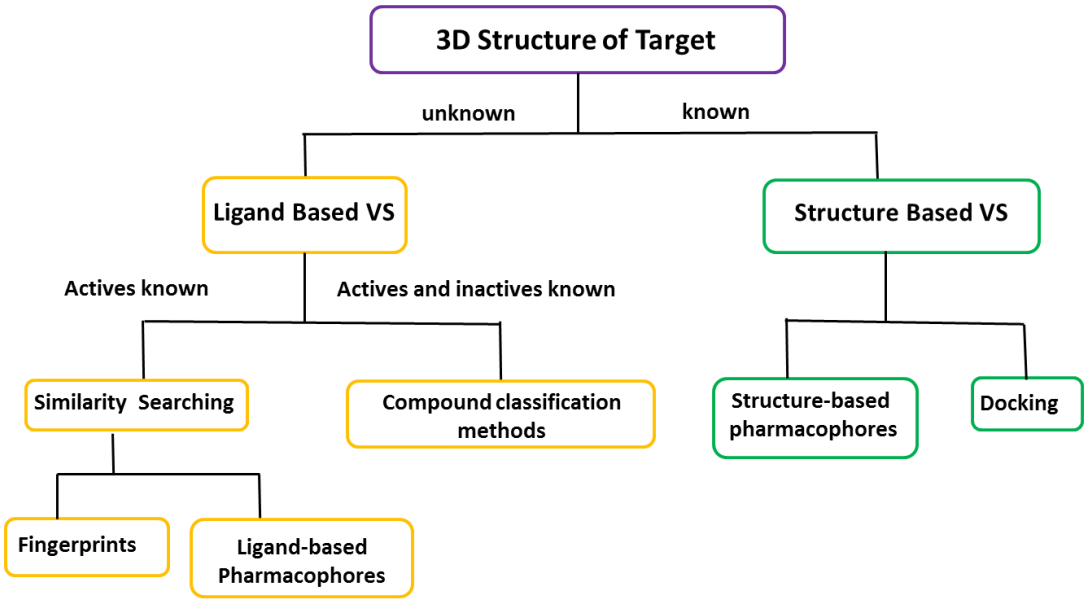

Figure 2.2. Classification of virtual screening methods.

2.3.2.1. Structure-based VS

Structure-based VS (SBVS) methods depend heavily on the availability of a 3D structure of the protein of interest [128,129]. Protein-ligand docking is the most traditional SBVS method, where compounds are docked, scored, and ranked according to the docking algorithm used [130,131].
In docking-based VS approach, often the top-ranked compounds are considered to be strong binders of the relevant macromolecular target and selected for further biological screening.

Successful application of docking-based VS campaigns depends on multiple factors including the quality of screening libraries, the conformation of the protein and the performance of scoring functions (see section **2.2**.).

In the current work, 3D molecular structures of the ligands were generated by Builder Module within the MOE. Next, ligands were energy-minimized using the MMFF94 force field [132-136] implemented in MOE. Protonation and tautomeric states at pH 7.4 were assigned by LigPrep [104] within the MAESTRO software package [137] of Schrodinger Suite 2012. Finally, the quality of screening libraries was assessed using different approaches discussed in section **2.3.1**.
Next, structure-based virtual screening of large compound libraries was executed using docking programs/software packages MOE, GOLD and GLIDE. The three scoring functions implemented in MOE; London dG, Affinity dG, and Alpha HB, the extra precision mode (GLIDE-XP) in GLIDE and the GoldScore algorithm in GOLD were used for ligand docking. The top-scored docking pose was kept for each ligand for further analysis. The predicted binding affinities of the molecules were then compared with the native (co-crystallized) inhibitors for each of the studied drug targets.

2.3.2.2. Pharmacophore-based VS

In the course of this work, we also assessed the similarity of two molecules by 3D fingerprints which are often referred to as pharmacophores. A pharmacophore is “the ensemble of steric and electronic features that is necessary to ensure the optimal molecular interactions with a specific biological target structure and to trigger (or to block) its biological response” [138].
The pharmacophore-based VS approaches can be classified into two;

- Ligand-based pharmacophore models are commonly used when the 3D structure of the target receptor is unknown [139]. It is based on the assumption that structurally similar molecules tend to have similar properties. In ligand-based approaches, the main goal is to rank a database of compounds according to their calculated similarity to the active reference compound. Ligand-based pharmacophores are used to determine
  - the overlap between the volume and surface matching,
  - the distance between the pharmacophoric features such as H-bond donors and acceptors, positive, negative charges, and aromatic moieties of two molecules [140].

- On the other hand, structure-based pharmacophore models are generally used when the 3D structure of the target receptor is known. 3D search queries reflect both the information about protein-ligand interactions (chemical features such as H-bond donors/acceptors, ionisable groups, and hydrophobic moieties are included) and the shape of the binding pocket (e.g. exclusion volumes were generated).

In the current work, structure-based pharmacophore model was the second method of choice for VS studies due to its outstanding advantages;

1. It is computationally inexpensive (thousands of molecules can be scored in a day),
2. It provides user defined protein flexibility (exclusion volumes can be tuned),
3. It is valid not only for the currently bound compound, but also unknown molecules,
4. It is easy to optimize (structural features can be added or removed).

In order to identify molecules similar to the co-crystallized ligands within the drug targets of interest, various structure-based pharmacophore models were generated using LigandScout software [141]. The performance of a pharmacophore model is often evaluated by its ability to discriminate between known actives from inactive compounds. Due to the absence of inactive datasets at the start of this project, we first generated decoy (supposed to be inactive) libraries using commercially available database; DUD-E (Directory of Useful Decoys) [142]. DUD-E decoy generation tool provides decoys with 1D physicochemical properties to those of the known actives but dissimilar 2D topology similar [143,144]. The motivation behind it was to avoid the artificial enrichment in validation/evaluation process of the pharmacophores. In the next step, Ligandscout software was used for pharmacophore generation and VS. Finally, the performance of each model was assessed by computing parameters such as enrichment factor, receiver operating characteristic–area under the curve (ROC-AUC), etc.

2.4. Molecular Dynamics Simulation

Molecular recognition and ligand binding are dynamic processes where atomic motions need to be taken into account. Using a single protein conformation obtained from NMR, X-ray crystallography or homology models provides only one state of motion of the structure rather than exploiting the ranges of flexibility of the macro/micro-molecule. In order to investigate the

behaviours of real molecules in motion, atomic forces that act on each atom in the system can be calculated and then the position of atoms can be moved following Newton's laws of motion to simulate the response of the system when using the Molecular Dynamics (MD) simulation approach.

MD simulations can be used in many applications:

a) Refining loop and side-chain conformations of derived homology models to get energetically favoured structures,
b) Elucidating all possible conformational states of proteins and identifying binding sites that cannot be attained from one rigid X-ray crystal structure,
c) Evaluating the stability of the ligands inside the putative binding site,
d) Extracting ensemble of multiple protein conformations as a virtual screening tool,
e) Calculating free-energies of bound and unbound ligand-protein complexes to understand the binding affinities of the corresponding small molecules [145].

In the current work, MD simulations were carried out using the program AMBER 12 [146] and the AMBER 2003 force field [147]. Atom types and AM1-BCC atomic charges [148] were generated for the ligand using the Antechamber module. Ligand parameters were obtained from the general AMBER force field GAFF [149]. Preparation of the ligand-protein complex, addition of counter ions, solvation, and preparation of parameter/topology and coordinate files were carried out using the LEaP module in AMBER. Parameters and libraries for zinc binding residues were defined as previously described [150]. The system was solvated using the water model TIP3BOX [151] and a margin of 10 Å. Two consecutive steps of minimization were carried out. In the first step 3,000 iterations (first 1,000 steepest descent and then 2,000 conjugate gradient) and in the second step 4,000 iterations (first 2,000 steepest descent and then 2,000 conjugate gradient) were applied to the system. In the first step, atom coordinates for the amino acid residues and ligand atoms were restrained to their initial coordinates with a force constant of 500 kcal $mol^{-1}Å^{-2}$ to relieve the unfavorable van-der-Waals contacts in the surrounding solvent. This step minimized the number of positions of the water molecules and ions. In the second step, restraints on atoms were removed and the whole system was minimized freely to relieve bad contacts in the entire system.

The temperature of the system was then equilibrated at 300 K through 100 ps of MD with a time step of 2 fs per step. A constant volume periodic boundary was set to equilibrate the temperature

of the system according to the Langevin dynamics [152] using a collision frequency of 1 ps^{-1} during the temperature equilibration routine. The protein and ligand atoms were restrained to the initial coordinates with a weak force constant of 10 kcal $mol^{-1}Å^{-2}$. The final coordinates obtained after temperature equilibration step were then used for a 20 ns MD routine during which the temperature was kept at 300 K by the Langevin dynamics using a collision frequency of 1 ps^{-1}. Constant pressure periodic boundary was used to maintain the pressure of the system at 1 bar using isotropic pressure scaling with a relaxation time of 2 ps. During the temperature equilibration and MD routines a non-bonded cut-off distance of 10 Å was used by applying the Particle Mesh Ewald (PME) method [153] to calculate the full electrostatic energy of the periodic system and the SHAKE algorithm [154] was used to adjust the constraints of all bonds involving hydrogen.

2.5. Binding Free Energy Calculations

Correct ranking of compounds according to their computed binding affinities remains an elusive goal in drug discovery. In contrast to molecular docking methods, free energy calculations take into account conformational changes upon binding and handle long-range electrostatics, desolvation of binding molecules, and entropic contributions better [155].

Binding free energy (BFE) methods can be broadly categorized into two classes; end-point methods and free energy pathway methods [155]. End-point methods only evaluate the initial and final states of the system whereas in pathway methods these two states are linked by a pathway that is broken into small steps. Pathway methods such as Free Energy Perturbation (FEP) and Thermodynamic Integration (TI) methods [156,157] are more computationally expensive than the end-point methods including the Linear Interaction Energy (LIE) [158], the Molecular Mechanics Poisson-Boltzmann Surface Area (MM-PBSA) and the Molecular Mechanics-Generalized Born Surface Area (MM-GBSA) methods [159].

Promising results have been obtained using the FEP and TI methods in the lead optimization phase. However, these methods are still rarely utilized in the stages of drug discovery, and this is mainly due to the demanding computational cost. On the other hand, several studies have reported the successful application of MM-PBSA and MM-GBSA methods for the estimation of protein-ligand binding affinities, and automated procedures have increased the applicability of these methods for a large compound selection [160-165]. Often, satisfactory correlations have

been acquired between the predicted binding affinities and the biological data, especially for ligand series with high structural similarity [162,166].

2.5.1. MM-PB(GB)SA Methods

In order to estimate the binding affinities of the inhibitors under study, we performed BFE calculations using the MM-PB(GB)SA method. The MM-PB(GB)SA approach combines molecular mechanics and continuum solvent models to predict the protein-ligand binding free energy. The binding strength of a ligand can be calculated as the difference between the free energy of the complex and the sum of the free energies of its components, the receptor and ligand **(eq1)**.

$$\textbf{(eq1)}\ \Delta G_{bind} = G_{complex} - (G_{receptor} + G_{ligand})$$

The total free energy of each component in eq1 can be computed as the sum of the gas-phase energy (E_{MM}), the solvation free energy (ΔG_{sol}) and the configurational entropy contributions ($-T\Delta S$) **(eq2)**.

$$\textbf{(eq2)}\ G_{molecule} = (E_{MM}) + (\Delta G_{sol}) - (T\Delta S)$$

E_{MM} energy is the molecular mechanics energy of the molecule that includes E_{int} (internal), E_{ele} (electrostatic), E_{vdw} (van der Waals) energies. The first E_{MM} energy term E_{int} treats bond, angle and dihedral energies, whereas the second E_{MM} energy term E_{ele} accounts for the Coulombic interactions between atoms occurring as a result of positive and negative partial atomic charges. The E_{vdw} term takes into account short and long ranged interactions among atoms. The component energy terms of E_{MM} energy were calculated using the *sander* module of AMBER. G_{sol} is the solvation energy term expressed as the sum of electrostatic solvation energy (polar contribution), $G_{PB/GB}$, and the non-electrostatic solvation energy (nonpolar contribution), and G_{SA} **(eq3)**. The polar solvation energy contribution was calculated by solving either Poisson-Boltzmann (PB) equation (MM-PBSA calculation) with the PBSA module or its variant Generalized Born (GB) equation (MM-GBSA calculation) with the MM-GBSA module in AMBER. Different GB models have been developed and implemented in AMBER such as GB^{HCT} (igb=1), GB^{OC1} (igb=2), GB^{OC2} (igb=5), and the more recently derived GBn models (igb=7, 8) [146,167-171]. In the current work we compared different MM-GBSA solvation models as well as the MM-PBSA method. The value of the implicit solvent dielectric constant

and the solute dielectric constant for GB calculations were set to 80 and 1, respectively. The solvent probe radius was set to 1.4 Å as default.

$$\textbf{(eq3)}\ \Delta G_{bind} = (E_{int} + E_{ele} + E_{vdw}) + (\Delta G_{PB/GB} + \Delta G_{SA}) - T\Delta S$$

The nonpolar solvation contribution is determined on the basis of a solvent-accessible surface area SASA solving equation 4 **(eq4)** where γ is a surface tension parameter and b, a parameterized value. Default values were used for γ and b terms.

$$\textbf{(eq4)}\ \Delta G_{SA} = \gamma\ SASA + b$$

The final binding energy is often determined by considering the conformational entropy change expressed as (– TΔS) where T is the absolute temperature and S the entropy of the molecule. Entropy of the molecule accounts for the loss of translational, rotational and conformational degrees of freedom of the ligand upon binding and it is critical for determining the absolute binding free energies when the ligand binding is driven by large favourable entropy changes [98,155,172]. However, it has already been reported that inclusion of entropy in calculations highly increases the computational cost, but did not always improve the accuracy [173]. It has also been shown that better correlations can be achieved upon omission of the entropy term from binding free energy calculations in case of congeneric series [166,173]. As we compared the relative binding free energies of a series of similar compounds, we did not include the entropic contribution in our calculations and only enthalpy values (ΔH) were computed to see whether a correlation could be achieved between binding enthalpies and biological data (IC_{50} values were converted into pIC_{50} values; $pIC_{50} = -\log IC_{50}$) **(eq5)**.

$$\textbf{(eq5)}\ \Delta H = (E_{MM}) + (\Delta G_{sol})$$

In addition, the estimation of conformational entropy change via the number of rotatable bonds in the ligand has been tested in docking and binding free energy calculations [164,174-179]. Promising results have been obtained implying that this measure may enhance the correlation with biological data [164,176]. The conformational entropy component was approximated from the number of rotatable bonds (NRot) of ligands **(eq6)** and combined with the enthalpy derived from MM-GBSA method and therefore this sum will be referred to as MM-GBSA values.

(eq6) $T\Delta S_{NRot}$ = number of rotatable bonds x 1.0 kcal/mol

In the current work, top-ranked docking poses were used for BFE calculations. Structurally conserved water molecules included for the docking studies were maintained during the geometry optimization of the complexes, but were removed for the binding free energy calculations. The protein-inhibitor complexes were first energy minimized and then equilibrated using a 100 ps MD run using the same parameters as described before. Three different systems were considered for the BFE calculations:

a) the protein-inhibitor complex which was energy minimized in explicit water,
b) 10 snapshots for each complex extracted evenly from the MD simulation and,
c) the final complex from the MD equilibration phase.

The binding free energy was then estimated using either the MM-PBSA or MM-GBSA module implemented in AMBER.

3. Aim of the Work

Sirtuins constitute a unique class of epigenetic enzymes that exist in a wide array of organisms ranging from bacteria to humans. Although sirtuins were first recognized as protein deacetylases, recent studies have shown that these enzymes can catalyze different post-translational modifications such as crotonylation, malonylation, succinylation, myristoylation, and ADP-ribosylation. Several studies have shown the complex regulatory role of sirtuins on various histones and non-histone proteins. Accordingly, sirtuin activity has been linked to the pathogenesis of viral and parasitic diseases, metabolic disorders, neurodegeneration, and cancer. Therefore, sirtuins are considered as attractive targets for drug discovery. The main goal of this work is to establish computer-based approaches to guide the development of potent and isoform selective modulators for these promising drug targets including sirtuins.

3.1. Development of a Time-efficient Post-docking Filter for Sirtuins

Due to the highly conserved amino acid sequence and the high structural similarity of the catalytic core between the members of the sirtuin family, it is challenging to identify selective drug-like inhibitors. In addition, sirtuins possess highly flexible substrate and cofactor binding sites. Thus, structure-based optimization of sirtuin modulators remains problematic.

In the first part of the work (**Manuscript 1**, [180]), we aimed to develop an *in silico* protocol that accurately predicts the binding affinities of sirtuin inhibitors before experimental testing. The protocol should derive significant correlations between the calculated scores and experimental data and thus, would reduce the time, cost and intricacy of hit identification and lead optimizations. In order to achieve this goal, it is important to validate the binding mode of compounds among sirtuin isoforms. Since the protein crystallization process is highly time-consuming and expensive, only a limited number of compounds can be solved with the relevant enzyme. Thus, as a first step, we focused on constructing a method to generate 3D structures for the overall inhibited conformation of sirtuins in a fast and accurate way. Second, we investigated the performance of different approaches ranging from simple scoring methods such as docking to more computationally demanding methods like binding free energy calculations.

3.2. Identification of Sirt2-selective Inhibitors

Up until now, several sirtuin modulators have been reported; however, most of these compounds lack potency, isoform-selectivity and/or drug-like physiochemical properties. Moreover, little is known about how these inhibitors bind to sirtuins. In the present work (**Manuscript 2**, [181]), we provide the first X-ray structures of Sirt2 in a complex with an isoform-selective drug-like inhibitor called SirReal2. We aimed to establish the structural basis of Sirt2-selective inhibition using computational methods and available sirtuin structures. To gain insights into the inhibition mechanism, Sirt2-SirReal2 complexes are compared with the available sirtuin structures in apo and ligand-bound conformations. To investigate the basis of SirReal2-mediated high-isotype selectivity, sequence and structural alignment should be performed within the members of sirtuin family. Assuming that SirReal2 binds to the other sirtuin subtypes in a similar fashion, the question whether minor sequence variations in the binding site have an impact on SirReal2 binding is explored using homology modeling and MD simulations.

3.3. Design of the First Photochromic Epigenetic Inhibitors

Despite its great potential, pharmacotherapy often suffers from a number of limitations such as: poor target selectivity and related side effects, and environmental toxicity and drug resistance. In this respect, photochromic compounds have recently gained much interest as they provide the possibility of a light-controlled reversibility to turn on and off enzymes [182]. Being a multivalent regulator of several physiological pathways, controlling the biological functions of sirtuins with small-molecules has great biomedical value. Therefore, the goal of this part of the work (**Manuscript 3**, [183]) was to prepare photochromic sirtuin inhibitors that are structurally related to an already known potent sirtuin inhibitor; Ro31-8220 (hSirt2; IC_{50} = 0.8 µM, [184]). We aimed to rationalize the observed *in vitro* activities and explain the isotype selective inhibition by carrying out docking studies on available Sirt1-3 structures and performing MM-GBSA calculations on single protein-inhibitor complexes.

3.4. Identification of Novel Inhibitors for smSirt2 of *Schistosoma mansoni*

According to the World Health Organization (WHO), 261 million people needed preventive treatment for schistosomiasis [185]. One of the main pathogens of schistosomiasis is the blood

fluke *Schistosoma mansoni* which encodes 5 sirtuins that are orthologs of human Sirt1, Sirt2, Sirt5, Sirt6 and Sirt7 [186]. Recently, human Sirt2 inhibitors were shown to be effective on both worm life span and reproduction [186]. In order to determine smSirt2 activity, we developed biochemical *in vitro* assays (**Manuscript 4**, [187]). These assays should enable us to screen large compound libraries and subsequent hit identifications. Considering the close sequence homology between schistosomal and human Sirt2, it was attractive to generate a homology model of the smSirt2 protein and to rationalize the interactions of the identified inhibitors.

3.5. Development and Evaluation of Virtual Screening Methods

Over the past decade, sirtuins have been shown to operate as both tumor promoters and tumor suppressors. To sort out biological functions of sirtuins in cancer and to gain in-depth understanding of the underlying mechanisms that result in contradictory activities, potent and isoform selective modulators of sirtuins are highly in need. Moreover, natural or natural product-related synthetic compounds constitute nearly half of the anticancer drugs that have reached the market from 1940s to 2010 [188]. Hence, we aimed to develop structure and ligand-based virtual screening methods that would enable the identification of potential anticancer agents from natural sources (**Manuscript 5** [189] and **Manuscript 6**). The potential of such methods was to be verified using the newly developed African natural product anticancer database (AfroCancer) and already known anticancer drug targets.

4. Results and Discussion

Book Chapter

Structure-based design and computational studies of sirtuin inhibitors

In: Epi-Informatics: Discovery and Development of Small Molecule Epigenetic Drugs and Probes Using Computational Approaches

Berin Karaman, Manfred Jung, Wolfgang Sippl

Ed. Jose Medina-Franco, Elsevier

Book: Epi-Informatics. MEDINA-FRANCO-9780128028087
(in press Nov. 2015)
Chapter: 11
http://dx.doi.org/10.1016/B978-0-12-802808-7.00011-3

Abstract

Histone deacetylases (HDACs) are enzymes that cleave acetyl groups from acetyl-lysine residues in histones and various non-histone proteins. Unlike the other three of the four classes of HDACs that have been identified in humans, which are zinc-dependent amidohydrolases, class III HDACs depend on nicotinamide adenine dinucleotide (NAD^+) for their catalytic activity. The seven members of the class III HDACs are also named sirtuins for their homology to Sir2p, a yeast histone deacetylase. Some sirtuin isoforms were found to be specific for other acyl modifications on the lysine side chain. Besides acetylation, modifications like propionylation, butyrylation, crotonylation, malonylation, succinylation, myristoylation, and 3-phosphoglycerylation have been recently detected. Sirtuin inhibitors have been critical for the linkage of sirtuin activity to many physiological and pathological processes, and sirtuin activity has been associated with the pathogenesis of cancer, HIV, and metabolic and neurological diseases. Presented here is an overview of the solved crystal structures of sirtuin subtpyes in complex with inhibitors, substrates and activators. The chapter also covers computer-based studies that resulted in the design and screening of novel sirtuin inhibitors representing useful chemical probes for studying the biological role of sirtuin isoforms.

Keywords: Histone deacetylase, sirtuins, docking, virtual screening, QSAR.

Manuscript 1

Docking and binding free energy calculations of sirtuin inhibitors

Berin Karaman and Wolfgang Sippl

European Journal of Medicinal Chemistry, 93, 584-598, **2015**

online available doi: 10.1016/j.ejmech.2015.02.045

Abstract

Sirtuins form a unique and highly conserved class of NAD^+-dependent lysine deacylases. Among these the human subtypes Sirt1-3 has been implicated in the pathogenesis of numerous diseases such as cancer, metabolic syndromes, viral diseases and neurological disorders. Most of the sirtuin inhibitors that have been identified so far show limited potency and/or isoform selectivity. Here, we introduce a promising method to generate protein-inhibitor complexes of human Sirt1, Sirt2 and Sirt3 by means of ligand docking and molecular dynamics simulations. This method highly reduces the complexity of such applications and can be applied to other protein targets beside sirtuins. To the best of our knowledge, we present the first binding free energy method developed by using a validated data set of sirtuin inhibitors, where both a fair number of compounds (33 thieno[3,2-*d*]pyrimidine-6-carboxamide derivatives) was developed and tested in the same laboratory and also crystal structures in complex with the enzyme have been reported. A significant correlation between binding free energies derived from MM-GBSA calculations and *in vitro* data was found for all three sirtuin subtypes. The developed MM-GBSA protocol is computationally inexpensive and can be applied as a post-docking filter in virtual screening to find novel Sirt1-3 inhibitors as well as to prioritize compounds with similar chemical structures for further biological characterization.

Keywords: Sirtuin, MM-GBSA, MM-PBSA, virtual screening.

Manuscript 2

Selective Sirt2 inhibition by ligand induced rearrangement of the active site

Tobias Rumpf, Matthias Schiedel, **Berin Karaman**, Claudia Roessler, Brian J. North, Attila Lehotzky, Judit Oláh, Kathrin I. Ladwein, Karin Schmidtkunz, Markus Gajer, Martin Pannek, Clemens Steegborn, David A. Sinclair, Stefan Gerhardt, Judit Ovádi, Mike Schutkowski, Wolfgang Sippl, Oliver Einsle, and Manfred Jung

Nature Communications, 6:6263, **2015**

online available: doi: 10.1038/ncomms7263

Abstract

Sirtuins are a highly conserved class of NAD^+-dependent lysine deacylases. The human isotype Sirt2 has been implicated in the pathogenesis of cancer, inflammation and neurodegeneration, which makes the modulation of Sirt2 activity a promising strategy for pharmaceutical intervention. A rational basis for the development of optimized Sirt2 inhibitors is lacking so far. Here we present high-resolution structures of human Sirt2 in complex with highly selective drug-like inhibitors that show a unique inhibitory mechanism. Potency and the unprecedented Sirt2 selectivity are based on a ligand-induced structural rearrangement of the active site unveiling a yet-unexploited binding pocket. Application of the most potent Sirtuin-rearranging ligand, termed SirReal2, leads to tubulin hyperacetylation in HeLa cells and induces destabilization of the checkpoint protein BubR1, consistent with Sirt2 inhibition in vivo. Our structural insights into this unique mechanism of selective sirtuin inhibition provide the basis for further inhibitor development and selective tools for sirtuin biology.

Manuscript 3

Chromo-pharmacophores: photochromic diarylmaleimide inhibitors for sirtuins

Carolin Falenczyk, Matthias Schiedel, **Berin Karaman,** Tobias Rumpf, Natascha Kuzmanovic, Morten Grøtli, Wolfgang Sippl, Manfred Jung, Burkhard Konig.

Chemical Science - Royal Society of Chemistry, 5, 4794-4799, **2014**

online available: doi: 10.1039/c4sc01346h

Abstract

Controlling the activity of sirtuins is of high biomedical relevance as the enzymes are involved in cancer, neurodegeneration and other diseases. Therefore structural elements of 3,4-bisindoylmaleimides (BIMs), which are known NAD^+-dependent histone deacetylase (sirtuin) inhibitors, were merged with photochromic diarylmaleimides to yield photoswitchable enzyme inhibitors. The new inhibitors show excellent photophysical properties, are switchable even in polar solvents, and subtype selective against hSirt2. The inhibitory activity changes up to a factor of 22 for the two photoisomers and physiological properties can therefore be effectively toggled by irradiation with light of different wavelengths. Docking experiments using the enzyme crystal structure explain the observed activity changes based on the steric demand of the thiophene substitution and the rigidity of the molecular structure.

Manuscript 4

Fluorescence-based screening assays for the NAD^+-dependent histone deacetylase smSirt2 from Schistosoma mansoni

Matthias Schiedel, Martin Marek, Julien Lancelot, **Berin Karaman**, Ingrid Almlöf, Johan Schultz, Wolfgang Sippl, Raymond J. Pierce, Christophe Romier, and Manfred Jung

Journal of Biomolecular Screening, 20(1), 112-121, **2015**

online available: doi: 10.1177/1087057114555307

Abstract

Sirtuins are NAD(+)-dependent histone deacetylases (HDACs) that cleave off acetyl but also other acyl groups from the ϵ-amino group of lysines in histones and other substrate proteins. Five sirtuin isoforms are encoded in the genome of the parasitic pathogen Schistosoma mansoni. During its life cycle, S. mansoni undergoes drastic changes in phenotype that are associated with epigenetic modifications. Previous work showed strong effects of hSirt2 inhibitors on both worm life span and reproduction. Thus, we postulate smSirt2 as a new antiparasite target. We report both the optimization of a homogeneous fluorescence-based assay and the development of a new heterogeneous fluorescence-based assay to determine smSirt2 activity. The homogeneous assay uses a coumarin-labeled acetyl lysine derivative, and the heterogeneous version is using a biotinylated and fluorescence-labeled oligopeptide. Magnetic streptavidin-coated beads allow higher substrate loading per well than streptavidin-coated microtiter plates and make it possible to screen for inhibitors of either smSirt2 or its human isoform (hSirt2) for selectivity studies. We also present hits from a pilot screen with inhibitors showing an IC_{50} lower than 50 μM. Binding of the hits to their targets is rationalized by docking studies using a homology model of smSirt2.

Keywords: Schistosoma mansoni; epigenetics; histone modifications; in vitro assay; sirtuin.

Manuscript 5

Molecular Modeling of Potential Anticancer Agents from African Medicinal Plants

Fidele Ntie-Kang, Justina Ngozi Nwodo, Akachukwu Ibezim, Conrad Veranso Simoben, **Berin Karaman**, Valery Fuh Ngwa, Wolfgang Sippl, Michael Umale Adikwu, and Luc Meva'a Mbaze

Journal of Chemical Information and Modeling, 54, 2433-50, **2014**

online available: doi: 10.1021/ci5003697

Abstract

Naturally occurring anticancer compounds represent about half of the chemotherapeutic drugs which have been put in the market against cancer until date. Computer-based or in silico virtual screening methods are often used in lead/hit discovery protocols. In this study, the "drug-likeness" of ∼400 compounds from African medicinal plants that have shown in vitro and/or in vivo anticancer, cytotoxic, and antiproliferative activities has been explored. To verify potential binding to anticancer drug targets, the interactions between the compounds and 14 selected targets have been analyzed by in silico modeling. Docking and binding affinity calculations were carried out, in comparison with known anticancer agents comprising ∼1 500 published naturally occurring plant-based compounds from around the world. The results reveal that African medicinal plants could represent a good starting point for the discovery of anticancer drugs. The small data set generated (named AfroCancer) has been made available for research groups working on virtual screening.

Manuscript 6

Pharmacophore Modeling and in Silico Toxicity Assessment of Potential Anticancer Agents from African Medicinal Plants

Fidele Ntie-Kang, Conrad Veranso Simoben, **Berin Karaman**, Valery Fuh Ngwa, Lydia Likowo Lifongo, Philip Neville Judson, Wolfgang Sippl, Luc Meva'a Mbaze

(Submitted work)

Abstract

Molecular modeling has been employed in the search for lead compounds for cancer chemotherapy. In this study, pharmacophore models have been generated and validated for use in virtual screening protocols for eight (8) known anticancer drug targets, including tyrosine kinase, protein kinase B (PKB β), cyclin-dependednt kinase (CDK), protein farnesyltransferase, human protein kinase, glycogen synthase kinase and indoleamine 2,3-dioxygenase 1. Pharmacophore models were validated through receiver operating characteristic (ROC) and Güner-Henry (*GH*) scoring methods, indicating that several of the models generated could be useful for the identification of potential anticancer agents from natural product databases. The validated pharmacophore models were used as 3D search queries for virtual screening of the newly developed AfroCancer database (~400 compounds from African medicinal plants), along with the NPACT dataset (comprising ~1,500 published naturally occurring plant-based compounds from around the world). Additionally, an *in silico* assessment of toxicity of the two datasets was carried out by use of eighty eight (88) toxicity end points predicted by Lhasa's expert knowledge-based system (Derek), showing that only an insignificant proportion of the promising anticancer agents would be likely to show high toxicity profiles. A diversity study of the two datasets, carried out using the analysis of principal components from the most important physicochemical properties often used to access drug-likeness of compound data sets, showed that the two data sets do not occupy the same chemical space.

Keywords: anticancer; natural products; medicinal plants; pharmacophore; toxicity; virtual screening.

5. Conclusion and Outlook

5. Conclusion and Outlook

Sirtuins are potential therapeutic targets which have been linked to the pathogenesis of metabolic disorders, viral and parasitic diseases, neurodegeneration and cancer. Hence, there is a growing interest in the regulation of sirtuin activity via small molecules with drug like properties. In the current work, we described *in silico* studies that would lead the development of novel sirtuin inhibitors. For this purpose, we applied various approaches including homology modeling, docking, molecular dynamic simulations, binding free energy calculations, and virtual screening.

5.1. Development of a Post-docking Filter: MM-GBSA Method

During the past two decades several series of sirtuin inhibitors have been identified, however, most of these compounds showed limited potency and isoform selectivity. Therefore, we addressed the issue of structure-based optimization of sirtuin inhibitors using a validated dataset of compounds, which showed potent Sirt1-3 inhibition.

Due to the absence of Sirt1 and Sirt2 crystal structures in complex with the inhibitors under study, we first generated protein-inhibitor complexes for each enzyme. We demonstrated that the correct bound conformation of the Sirt isoforms could be employed in a fast and accurate way by means of ligand docking and applying a short MD simulation. This method:

- can be applied to other protein targets beside sirtuins,
- reduces the complexity of applications such as homology modeling which requires expertise,
- and is limited to the availability of a 3D structure with close conformation to the homolog protein of interest.

We observed that the applied docking protocol was able to correctly reproduce the binding mode of the inhibitors, however, no correlation could be attained between the docking scores and biological data (R^2 = 0.26 for Sirt1, R^2 = 0.18 for Sirt2 and R^2 = 0.16 for Sirt3). Since docking algorithms of today do not take solvation effects and protein flexibility into account, they often fail to predict the binding affinity of compounds accurately. Thus, in the next step, we explored the performance of more sophisticated methods such as binding free energy (BFE) calculations.

Based on the obtained results from MM-PB(GB)SA calculations, the following conclusions can be made:

- A small number of frames retrieved from MD simulations provide a significant correlation with the experimental data.

  We observed a better performance of the BFE methods when we used a small collection of protein-ligand complexes instead of one single conformation retrieved after energy minimization or MD simulation. The possible reasons behind this observation could be:
  - the enlarged conformational space covered during MD resulted in complexes where ligands show a better fit to the protein,
  - averaging the binding energies retrieved from a small collection of protein-inhibitor complexes alleviated the error that comes from the energy terms which are sensitive to the exact position of the ligand in the binding (e.g. the vdW term).
- Among all different implicit solvation models tested, the best overall performance was observed using the GB-1 solvation model (R^2 = 0.79 for Sirt1, R^2 = 0.76 for Sirt2 and R^2 = 0.60 for Sirt3). We also found that the MM-GBSA method pursued with a fairly new and not well studied GB-8 solvation model, gives promising results (R^2 = 0.69 for Sirt1, R^2 = 0.72 for Sirt2 and R^2 = 0.57 for Sirt3).
- We determined a general improvement in the accuracy of binding poses when all the docking poses were considered and ranked by enthalpy values in comparison to the top-ranked docking pose. However, the lowest binding energy pose was not always the closest match to the crystal structure.
- We tested whether we could get better correlation between biological data and enthalpy values upon using the lowest binding free energy pose instead of the top-ranked docking pose. We observed only a slight increase of R^2 from 0.60 to 0.62 and q^2_{LOO} from 0.54 to 0.56.
- Addition of entropy term with a simplified approach where the number of rotatable bonds is taken into account did not improve the overall performance of the MM-GBSA approach. Being computationally demanding and time consuming, normal mode analysis was not tested to assess the entropic contribution in this work. Therefore, whether including such methods into the MM-GBSA workflow will increase the overall performance has yet to be explored in the future.

- Since the CPU time required for calculation of one inhibitor takes around 10 min, the MM-GBSA approach would not be feasible to screen large compound libraries and instead can only be used as a post-docking filter.

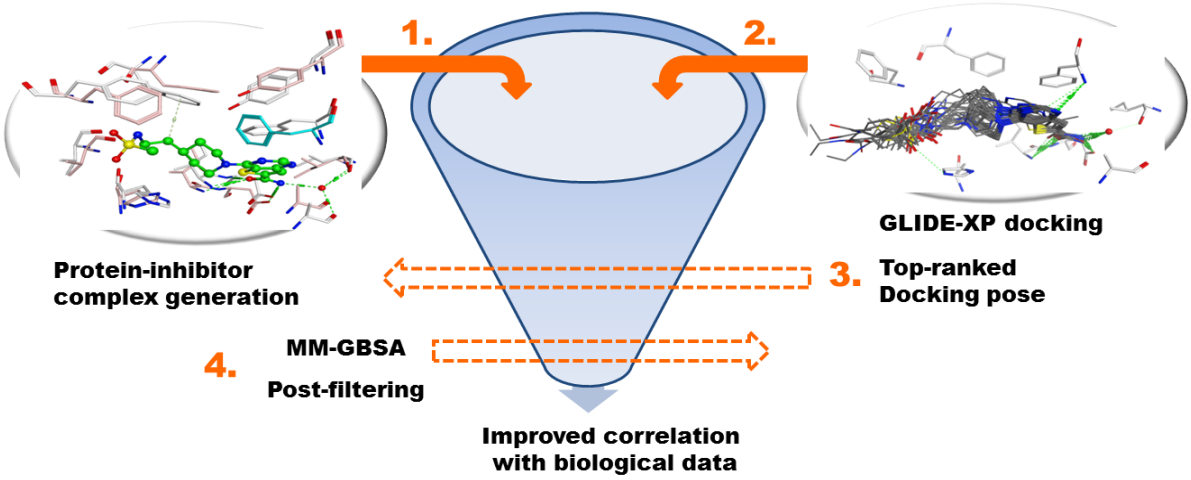

Figure 5.1. Workflow used in the development of post-docking filter for sirtuins. Adapted from [180].

In summary, the established MM-GBSA protocol (**Figure 5.1.**) is computationally inexpensive and can be applied as a post-docking filter in virtual screening campaigns to identify novel sirtuin inhibitors. Given the fact that this method is designed and validated for structure-based optimization of inhibitors with similar chemical structures, one should be cautious if it could be applied for datasets that cover a large chemical space. We recommend utilizing ensemble docking methodologies as a docking protocol which would enhance the conformational space covered and thus, enable a better prediction of the binding mode and affinity for each compound.

5.2. Structural Basis of Sirt2-selective Inhibition

Three critical issues have to be fulfilled in order to validate sirtuins as therapeutic targets:

1. Identification of potent and subtype selective sirtuin modulators to identify the targets of sirtuin family members and thus, their key roles in physiological pathways,
2. Foundation of structural basis for subtype selectivity (e.g. crystallization of identified modulators with the target),

3. Structure-based optimization of compounds in order to obtain drug-like molecules with optimized potency and physicochemical properties for further testing in animal models.

In this part of the work, we establish the structural basis of Sirt2-selective inhibition with newly identified SirReal inhibitors. Among those, SirReal2 showed high selectivity for Sirt2 (IC_{50} = 140 nM), while only a slight inhibition of Sirt1 (22% inhibition at 100 µM) and Sirt6 (19% inhibition at 200 µM) could be detected. Furthermore, no significant effects were seen against the sirtuin isotypes Sirt3-5 and the classical HDACs; HDAC1 and HDAC6. Due to the lack of a suitable screening assay for human Sirt7, the *in vitro* inhibition could not be measured for this isoform. In order to rationalize the structure activity/selectivity relationship of SirReals, X-ray crystal structures of SirReal2 were solved in the presence of substrate (**Figure 5.2.**) and cofactor NAD^+.

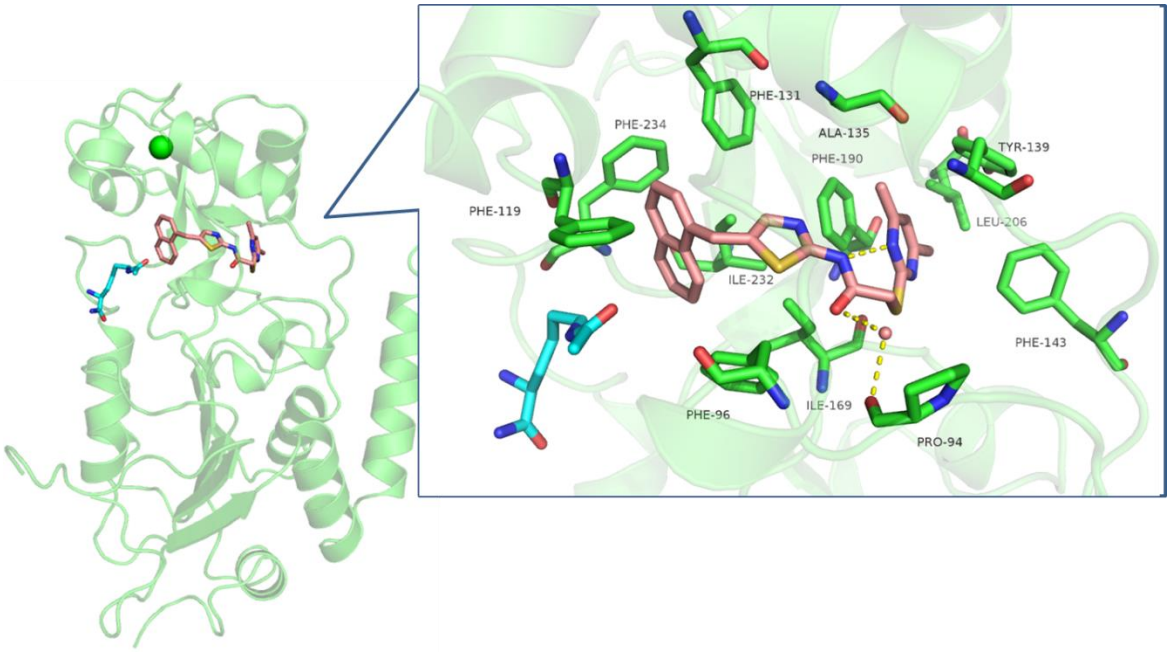

Figure 5.2. Crystal structure of Sirt2 in complex with SirReal2 and an acetyl-lysine peptide derived from histone H3, (PDB; 4RMH). The structure of Sirt2 and the zinc ion is shown as green cartoon model and sphere, respectively. Molecular structures of SirReal2 and substrate are illustrated as pink and cyan sticks, respectively. A closer look of the binding site of the ligands is shown in the box. Only the interacting protein residues are shown as green sticks, the bridging water molecule is displayed as pink ball and hydrogen bonds are depicted as yellow dashed lines.

To get insights into the inhibition mechanism, we first compared the X-ray structures of Sirt2-SirReal2 with the available sirtuin structures in apo and ligand-bound conformations. Next, we

explored the basis of high-isotype selectivity against Sirt2. For this purpose, sequence and structural alignments were done among the members of sirtuin family. We observed that Sirt4-6 exhibit substantial structural and amino acid sequence differences in their deacylases domain in comparison to Sirt2. Such differences were highly prominent especially in the SirReal2 binding pocket, rationalizing the observed lack of inhibitory effect on Sirt4-6 by SirReal2. On the other hand, Sirt1 and Sirt3, which are phylogenetically more closely related to Sirt2, exhibit minor sequence variations. We observed that Sirt1/3 apo (open conformation) structures are also more similar to the Sirt2-SirReal2 complexes than the apo structures of Sirt5/6. We generated homology models (HMs) of Sirt1 and Sirt3 to investigate whether these enzymes are able of forming a similar allosteric binding pocket as seen in Sirt2-SirReal2 crystal structures. If so, we wanted to explore whether the minor sequence variations within the active cleft of Sirt1/3 have an impact on SirReal2 binding. To rationalize the SirReal2 binding in Sirt1/3 homology models, we performed docking studies in the next step.

Based on the observed results obtained in this work, the following conclusions can be made:

- SirReals rearranges the Sirt2 active site and behave as allosteric inhibitors.
  - Structural alignment of Sirt2-SirReal2 complexes with the available Sirt2 structures (apo- and holo-) showed that the zinc binding domain in Sirt2-SirReal2 structures adopts an open conformation similar to the one in Sirt2-apo.
  - In the previously solved sirtuin structures, a “closure” of the active cleft was observed upon binding of a substrate or a pseudo-substrate. This closure induces the zinc binding domain rotation against the Rossmann fold domain and helps to correctly orientate the acetyllysine in the hydrophobic tunnel. In SirReal2-inhibited Sirt2 structures no closure of the substrate channel was observed, even in the presence of a substrate.
  - The rearrangement in the acetyl-lysine channel does not prevent the binding of peptide substrate. However, the bulky naphthyl moiety of SirReal2 forces the acetyl-lysine ~ 5Å out of its physiological position.
  - Collectively, these results suggest that, SirReal2 traps Sirt2 in an intermediate state between apo, “open conformation”, and substrate bound, “closed conformation” which is named as “open-locked conformation”. This unique conformation does not

enable the correct orientation of the peptide substrate and prevents the deacetylation reaction. These findings rationalize the inhibition mechanism of SirReals.

- Selective inhibition of Sirt2 by SirReal2 results from Sirt2-specific amino acid network.
  - The dimethylpyrimidine (DMP) substituent of SirReal2 induces the formation of the "selectivity pocket" which is located deep inside the catalytic cavity above the C-pocket. Sirtuin isotypes (Sirt1-6) exhibit major differences in their amino acid sequence, particularly in their "selectivity pocket".
  - Homology models of Sirt1 and Sirt3 provided evidence that even minor sequence variations in the catalytic domain result in major shape and surface changes in SirReal2 binding pocket. In the case of Sirt1, these mutations were mainly localized in the binding pockets of the naphthyl and aminothiazole moieties, resulting in a tighter extended C pocket. However, in case of Sirt3, these mutations were mainly localized in the binding pocket of DMP, resulting in a larger and solvent-accessible selectivity pocket.
  - Docking of SirReal2 into Sirt1/3 HMs resulted in less favorable docking scores in comparison to the docking poses of SirReal2 into the Sirt2-SirReal2 complexes. The reasons behind the poor score are:
    - ❖ the unfavorable orientation of SirReal2 and the loss of van der Waals interactions due to the residue mutations and structural differences in the active cleft of Sirt1 and Sirt3 HMs,
    - ❖ loss of an intramolecular hydrogen bond between the amide of the aminothiazole and nitrogen atom of the DMP moiety which gives SirReal2 a rigid form and provides an ideal complementary shape in the active site of Sirt2.

In conclusion, the mutations and reorientation of residues in the deacetylase domain of sirtuin subtypes result in substantial structural differences in the active cleft. These differences are highly pronounced in the newly discovered allosteric binding pocket of Sirt2 that is formed upon SirReal2 binding. Thus, this pocket can be targeted to design selective sirtuin inhibitors in the future. Moreover, the newly developed MM-GBSA method can be applied for the structure-based optimization of SirReals.

5.3. Identification of Potent and Sirt2-selective Photochromic Inhibitors

Sirtuins have been linked to the pathogeneses of several diseases such as cancer, neurodegeneration, and metabolic disorders. Therefore, it is important to regulate the activity of sirtuins to investigate their role in cellular processes. Introducing photochromic properties to the scaffold of an already known ligand represent one such strategy to control the activity of the enzymes by light. In order to develop presumably photoswitchable sirtuin inhibitors, we merged the structure of photochromic diarylmaleimides with the pharmacophore of the known sirtuin inhibitor, Ro31-8220 (hSirt2; IC_{50} = 0.8 µM, [184]) (**Figure 5.3.**).

The new compounds exhibited potent and Sirt2 selective photochromic inhibitors. Among those, compound **11** (**Figure 5.3.**) showed the optimal photochromic and Sirt2 inhibition (open photoisomer; IC_{50} = 4.2 µM, closed photoisomer; IC_{50} = 92.3 µM) properties:

- Photoisomers of **11** differ more than 20 fold in their inhibition ability which allows the remote control of the enzyme activity with green light,
- Neither the open isomer, nor the closed isomer of **11** showed Sirt1 and Sirt3 inhibitory effect under the same assay conditions, confirming its isotype selective inhibition of Sirt2,
- Photochemical conversion of the closed photoisomer to the open photoisomer of **11** is possible in polar solvents which is essential for biological appliations

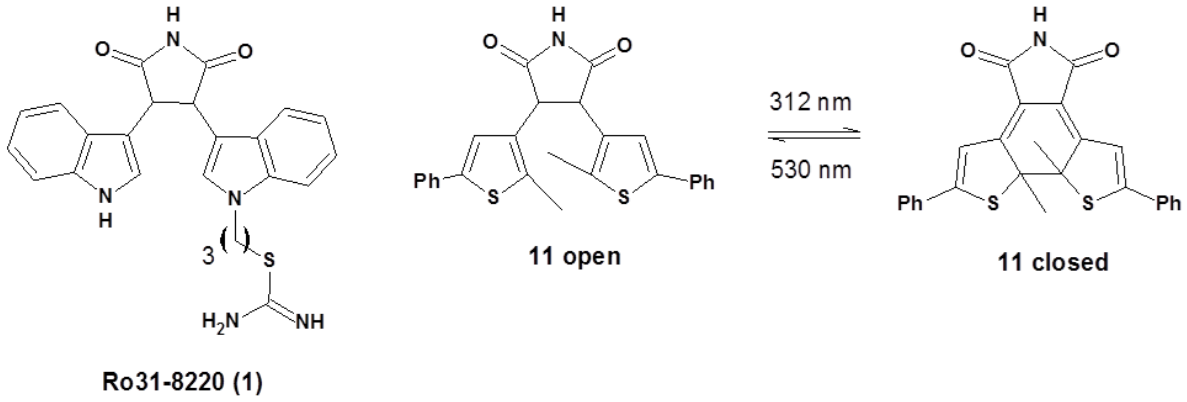

Figure 5.3. Known sirtuin inhibitor **1** (Ro31-8220) and the structurally related photochromic diarylmaleimide **11** in open and closed photoisomers. Adapted from [183].

Docking studies of diarylmaleimide inhibitors into the available Sirt1-3 structures were able to explain the Sirt2 inhibition mechanism and also established the basis of structure activity-selectivity relationship. Based on the docking results obtained in this work, the following conclusions can be made:

- Diarylmaleimide inhibitors occupy the acetyllsine pocket of Sirt2 and make H-bond interactions with the conserved residue Val233 (Sirt2 numbering). Thus, maleimides block the binding of acetyllysine substrate and inhibit the deacetylation mechanism.
- The photochemical conversion from the open isomer to the closed isomer of diarylmaleimides results in an inhibitory activity loss up to 22 factor. The observed activity changes are based on the increase in the steric demand and the rigidity of the molecular structure upon ring closure, resulting in unfavorable orientation of the molecular structure and/or loss of H-bond interaction with Val233.
- The different orientations of the amino acid residues in the acetyllysine channel of Sirt1 and Sirt3 structures restrict the interaction of maleimides in the binding pocket, rationalizing the observed selectivity of photochromic inhibitor **11**.

In conclusion, the newly discovered compounds represent the first photochromic sirtuin inhibitors reported in the literature. These compounds show Sirt2 selective inhibition with regard to the Sirt1 and Sirt3 isoforms. However, to elucidate whether these compounds solely inhibit Sirt2 isoform or not, further testing has to be done against other members of sirtuin family including Sirt4-7. Moreover, *in vitro* competition assays against substrate peptide can be carried out to confirm the proposed binding pocket for diarylmaleimides. Based on the docking results a structure-based optimization of these inhibitors can be accomplished as a next step. In addition, we expect that the application of this concept, merging different chromophoric groups with the pharmacophores of already known inhibitors, would lead the identification of novel photochromic sirtuin inhibitors in the near future.

5.4. Identification of Novel Inhibitors for smSirt2 of *Schistosoma mansoni*

Schistosomiasis is considered as one of the ‘neglected tropical diseases’ caused by parasitic worms. Emerging number of people are affected each year fom schistosomiasis. Praziquantel is currently the only antischistosomal agent used to control this disease and thus, there is an urgent

need for the development of alternative therapeutics. Given the fact that hSirt2 inhibitors showed strong effects on both the life span and reproduction of *S. mansoni* [186], the main pathogen of schistomiasis, we screened our inhouse sirtuin inhibitors to search for novel smSirt2 inhibitors.

First, two complementary *in vitro* assays were developed to determine the activity of smSirt2. Initial screens were conducted with a high-throughput fluorescence-based homogeneous assay which is suitable for screening large compound libraries in a cost-efficient manner. We tested 230 compounds consisting of nicotinamide analogs and adenosine mimetics and identified nine novel smSirt2 inhibitors with an inhibition higher than 50% at 100 µM. Since homogeneous assays can produce false positive results due to the interference by fluorescent compounds, in the next step, we counter-screened the identified smSirt2 inhibitors by using more costly heterogeneous assay protocol. We could characterize 5 compounds, including the kinase inhibitor Vatalanib (smSirt2, IC_{50} = 12 µM, **Figure 5.4.**), with an IC_{50} value ranging from 8 µM to 37 µM. Due to the absence of a 3D structure of smSirt2, we generated a homology model of this enzyme. We could rationalize the interaction of the identified inhibitors with smSirt2-HM by means of docking (as an example docked pose of Vatalanib, **Figure 5.4.**).

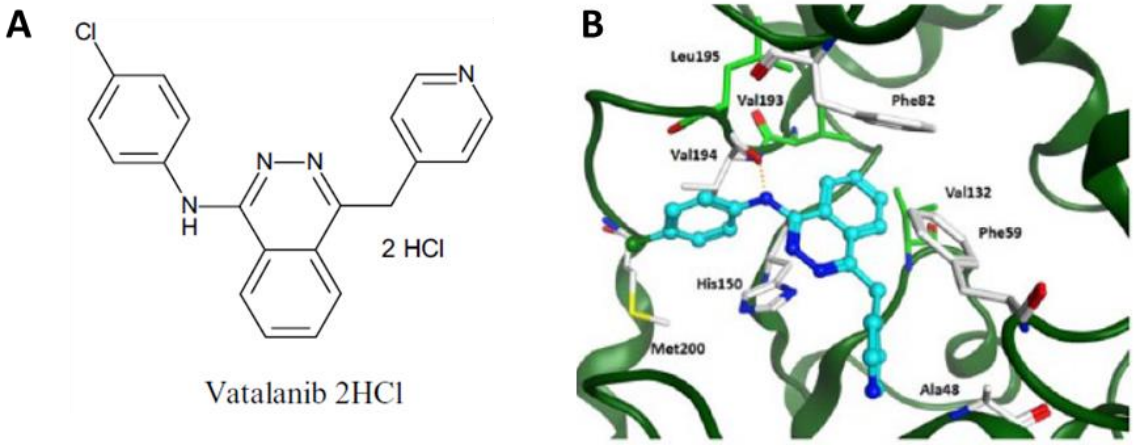

Figure 5.4. Novel inhibitor of smSirt2; Vatalanib 2HCl. **A)** Molecular structure of Vatalanib 2HCl. **B)** Homology model of smSirt2 (dark green ribbon) in a complex with docked Vatalanib (cyan ball and sticks). Only interacting amino acid residues (white sticks) are shown for clarity. Residues that are different in the smSirt2 acetyl lysine tunnel compared to human Sirt2 are shown as green sticks. Adapted from [187].

In general, the *in vitro* assay protocol presented in this work is a valuable tool to screen larger compound libraries to identify novel smSirt2 inhibitors. Moreover, *in silico* virtual screening campaigns based on our smSirt2 homology model can be harmonized with the biochemical assays to increase the time-cost efficiency and to maximize the chemical space covered. Given the fact that schistosomal and human sirtuins are closely related orthologs, it is important to attain selectivity over human sirtuins. Thus, the focal point of the next step would be structure-based optimization of the hits to obtain smSirt2 selective inhibitors.

5.5. Development and Evaluation of Virtual Screening Methods

According to the World Health Organization (WHO), annual cancer cases are expected to rise from fourteen (in 2012) to twenty-two million within the next 20 years [190]. Yet, natural or natural product-related synthetic compounds comprise half of the anticancer drugs which have reached the market in the last seventy years [191]. Due to their complex regulatory role in cell proliferation and viability, sirtuins have spurred great interest in the field of anticancer research. However, potent and isoform selective sirtuin modulators are still lacking and thus, probing biological functions of sirtuins in cancer remains as an elusive goal.

5.5.1. Generation of AfroCancer Dataset

In this context, we first collected ~ 400 compounds (AfroCancer database) from the literature analyses which have been isolated from African medicinal plants. Then, we evaluated the drug-likeness properties of these compounds using Lipinski's rule of five [126]. We observed that newly developed AfroCancer dataset has enhanced drug-likeness properties in comparison to the known Naturally Occurring Plant-based Anticancer Compound-Activity-Target (NPACT) [192] and Dictionary of Natural Products (DNP) [193]. Moreover, we calculated a set of ADMET-related properties of this library to detect compounds with limited drug-like properties. Principal component analysis performed on the NPACT and AfroCancer datasets revealed that these two libraries do not occupy the same chemical space, implying the presence of novel scaffolds in the AfroCancer dataset.

5.5.2. Structure- and ligand-based VS Approaches

In the next step, we established a structure-based VS method to detect the presence of potential anticancer agents within the AfroCancer dataset. For this purpose, we carried out docking studies using different scoring functions on fourteen selected known anticancer drug targets (as an example, the androgen receptor in a complex with co-crystallized 9α-fluorocortisol, PDB ID; 1GS4, **Figure 5.5.**). A significant proportion of the dataset acquired comparable docking scores and target interactions in comparison to the native ligands bound within the anticancer drug targets (**Figure 5.5.**).

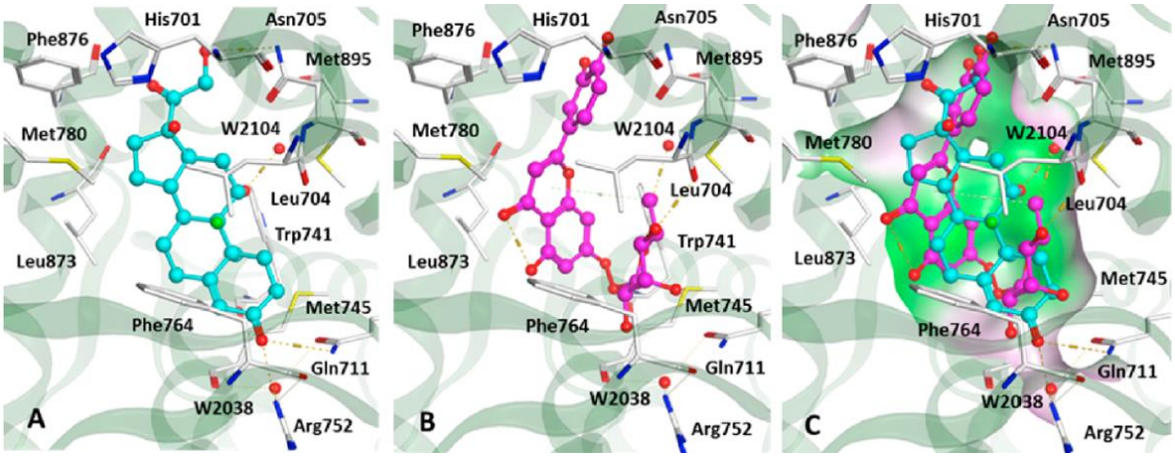

Figure 5.5. Glide docking of AfroCancer Dataset. **A)** Crystal structure of the androgen receptor (dark green ribbon) in complex with co-crystallized 9α-fluorocortisol (cyan ball and sticks) (PDB ID; 1GS4). **B)** Docking pose of luteolin-7-O-β-glucopyranoside (pink ball and sticks) onto the androgen receptor. **C)** Comparison of the co-crystallized 9α-fluorocortisol and the docked luteolin-7-O-β-glucopyranoside. Only interacting amino acid residues (white sticks) are shown for clarity. Water molecules and hydrogen bonds are shown as red spheres and dashed lines, respectively. The molecular surface of the binding pocket is displayed and colored according to the hydrophobicity. Polar regions are shown in magenta, hydrophobic regions in green. Adapted from [189].

Moreover, we generated and validated pharmacophore-based VS models based on the known eight anticancer drug targets. These pharmacophore models were subsequently applied on the NPACT and AfroCancer datasets. We observed higher pharmacophore fit scores and hit rates in the case of AfroCancer dataset, indicating the potential of this dataset to search for naturally occurring anticancer agents.

In conclusion, the newly developed AfroCancer dataset represent a good starting point for the discovery of anticancer agents. Although a significant number of the compounds in the dataset fulfill the drug-likeness criteria, some of them were predicted to be toxic. In order to evaluate the performance of structure- and ligand-based VS models presented in this work, predicted hits need to be experimentally tested. Docking- and pharmacophore-based VS methods have shown to be vauable tools for hit identification, nevertheless, these scoring methods often do not reflect the biological activity of the compounds. Therefore, we recommend post-processing of virtual screening results with more sophisticated rescoring methods such as MM-GBSA method.

6. References

[1] Dhanak, D., Cracking the code: the promise of epigenetics. *ACS Med Chem Lett* **2012,** *3* (7), 521-3.

[2] Egger, G.; Liang, G.; Aparicio, A.; Jones, P. A., Epigenetics in human disease and prospects for epigenetic therapy. *Nature* **2004,** *429* (6990), 457-63.

[3] Feinberg, A. P.; Vogelstein, B., Hypomethylation distinguishes genes of some human cancers from their normal counterparts. *Nature* **1983,** *301* (5895), 89-92.

[4] Cooper, G. M.; Hausman, R. E., *The Cell: A Molecular Approach*. 4th edition ed.; Sinauer Associates.

[5] Jenuwein, T.; Allis, C. D., Translating the Histone Code. *Science* **2001,** *293* (5532), 1074-1080.

[6] Thiagalingam, S.; Cheng, K. H.; Lee, H. J.; Mineva, N.; Thiagalingam, A.; Ponte, J. F., Histone deacetylases: unique players in shaping the epigenetic histone code. *Ann N Y Acad Sci* **2003,** *983*, 84-100.

[7] de Ruijter, A. J.; van Gennip, A. H.; Caron, H. N.; Kemp, S.; van Kuilenburg, A. B., Histone deacetylases (HDACs): characterization of the classical HDAC family. *Biochem J* **2003,** *370* (Pt 3), 737-49.

[8] Haigis, M. C.; Sinclair, D. A., Mammalian sirtuins: biological insights and disease relevance. *Annu Rev Pathol* **2010,** *5*, 253-95.

[9] Mottamal, M.; Zheng, S.; Huang, T. L.; Wang, G., Histone Deacetylase Inhibitors in Clinical Studies as Templates for New Anticancer Agents. *Molecules* **2015,** *20* (3), 3898-3941.

[10] Haberland, M.; Montgomery, R. L.; Olson, E. N., The many roles of histone deacetylases in development and physiology: implications for disease and therapy. *Nat Rev Genet* **2009,** *10* (1), 32-42.

[11] Hamm, C. A.; Costa, F. F., Epigenomes as therapeutic targets. *Pharmacol Ther* **2015,** *151*, 72-86.

[12] Abend, A.; Kehat, I., Histone deacetylases as therapeutic targets--from cancer to cardiac disease. *Pharmacol Ther* **2015,** *147*, 55-62.

[13] Sauve, A. A., Sirtuin chemical mechanisms. *Biochim Biophys Acta* **2010,** *1804* (8), 1591-603.

[14] North, B. J.; Verdin, E., Sirtuins: Sir2-related NAD-dependent protein deacetylases. *Genome Biol* **2004,** *5* (5), 224.

[15] Sanders, B. D.; Jackson, B.; Marmorstein, R., Structural basis for sirtuin function: what we know and what we don't. *Biochim Biophys Acta* **2010,** *1804* (8), 1604-16.

[16] Parenti, M. D.; Bruzzone, S.; Nencioni, A.; Del Rio, A., Selectivity hot-spots of sirtuin catalytic cores. *Mol Biosyst* **2015**.

[17] Borra, M. T.; Langer, M. R.; Slama, J. T.; Denu, J. M., Substrate specificity and kinetic mechanism of the Sir2 family of NAD+-dependent histone/protein deacetylases. *Biochemistry* **2004,** *43* (30), 9877-87.

[18] Cosgrove, M. S.; Bever, K.; Avalos, J. L.; Muhammad, S.; Zhang, X.; Wolberger, C., The structural basis of sirtuin substrate affinity. *Biochemistry* **2006,** *45* (24), 7511-21.

[19] Avalos, J. L.; Bever, K. M.; Wolberger, C., Mechanism of sirtuin inhibition by nicotinamide: altering the NAD(+) cosubstrate specificity of a Sir2 enzyme. *Mol Cell* **2005,** *17* (6), 855-68.

[20] Bao, X.; Wang, Y.; Li, X.; Li, X. M.; Liu, Z.; Yang, T.; Wong, C. F.; Zhang, J.; Hao, Q.; Li, X. D., Identification of 'erasers' for lysine crotonylated histone marks using a chemical proteomics approach. *Elife* **2014,** *3*.
[21] Teng, Y.-B.; Jing, H.; Aramsangtienchai, P.; He, B.; Khan, S.; Hu, J.; Lin, H.; Hao, Q., Efficient Demyristoylase Activity of SIRT2 Revealed by Kinetic and Structural Studies. *Sci. Rep.* **2015,** *5*.
[22] Jiang, H.; Khan, S.; Wang, Y.; Charron, G.; He, B.; Sebastian, C.; Du, J.; Kim, R.; Ge, E.; Mostoslavsky, R.; Hang, H. C.; Hao, Q.; Lin, H., SIRT6 regulates TNF-alpha secretion through hydrolysis of long-chain fatty acyl lysine. *Nature* **2013,** *496* (7443), 110-3.
[23] Du, J.; Zhou, Y.; Su, X.; Yu, J. J.; Khan, S.; Jiang, H.; Kim, J.; Woo, J.; Kim, J. H.; Choi, B. H.; He, B.; Chen, W.; Zhang, S.; Cerione, R. A.; Auwerx, J.; Hao, Q.; Lin, H., Sirt5 is a NAD-dependent protein lysine demalonylase and desuccinylase. *Science* **2011,** *334* (6057), 806-9.
[24] Feldman, J. L.; Baeza, J.; Denu, J. M., Activation of the protein deacetylase SIRT6 by long-chain fatty acids and widespread deacylation by mammalian sirtuins. *J Biol Chem* **2013,** *288* (43), 31350-6.
[25] Feldman, J. L.; Dittenhafer-Reed, K. E.; Kudo, N.; Thelen, J. N.; Ito, A.; Yoshida, M.; Denu, J. M., Kinetic and Structural Basis for Acyl-Group Selectivity and NAD Dependence in Sirtuin-Catalyzed Deacylation. *Biochemistry* **2015**.
[26] Bao, J.; Lu, Z.; Joseph, J. J.; Carabenciov, D.; Dimond, C. C.; Pang, L.; Samsel, L.; McCoy, J. P., Jr.; Leclerc, J.; Nguyen, P.; Gius, D.; Sack, M. N., Characterization of the murine SIRT3 mitochondrial localization sequence and comparison of mitochondrial enrichment and deacetylase activity of long and short SIRT3 isoforms. *J Cell Biochem* **2010,** *110* (1), 238-47.
[27] Scher, M. B.; Vaquero, A.; Reinberg, D., SirT3 is a nuclear NAD+-dependent histone deacetylase that translocates to the mitochondria upon cellular stress. *Genes Dev* **2007,** *21* (8), 920-8.
[28] Stunkel, W.; Campbell, R. M., Sirtuin 1 (SIRT1): the misunderstood HDAC. *J Biomol Screen* **2011,** *16* (10), 1153-69.
[29] Kaeberlein, M.; Kirkland, K. T.; Fields, S.; Kennedy, B. K., Sir2-independent life span extension by calorie restriction in yeast. *PLoS Biol* **2004,** *2* (9), E296.
[30] Dang, W.; Steffen, K. K.; Perry, R.; Dorsey, J. A.; Johnson, F. B.; Shilatifard, A.; Kaeberlein, M.; Kennedy, B. K.; Berger, S. L., Histone H4 lysine 16 acetylation regulates cellular lifespan. *Nature* **2009,** *459* (7248), 802-7.
[31] Li, Y.; Xu, W.; McBurney, M. W.; Longo, V. D., SirT1 inhibition reduces IGF-I/IRS-2/Ras/ERK1/2 signaling and protects neurons. *Cell Metab* **2008,** *8* (1), 38-48.
[32] Bauer, J. H.; Goupil, S.; Garber, G. B.; Helfand, S. L., An accelerated assay for the identification of lifespan-extending interventions in Drosophila melanogaster. *Proc Natl Acad Sci U S A* **2004,** *101* (35), 12980-5.
[33] Howitz, K. T.; Bitterman, K. J.; Cohen, H. Y.; Lamming, D. W.; Lavu, S.; Wood, J. G.; Zipkin, R. E.; Chung, P.; Kisielewski, A.; Zhang, L. L.; Scherer, B.; Sinclair, D. A., Small molecule activators of sirtuins extend Saccharomyces cerevisiae lifespan. *Nature* **2003,** *425* (6954), 191-6.
[34] Milne, J. C.; Lambert, P. D.; Schenk, S.; Carney, D. P.; Smith, J. J.; Gagne, D. J.; Jin, L.; Boss, O.; Perni, R. B.; Vu, C. B.; Bemis, J. E.; Xie, R.; Disch, J. S.; Ng, P. Y.; Nunes, J. J.; Lynch, A. V.; Yang, H.; Galonek, H.; Israelian, K.; Choy, W.; Iffland, A.; Lavu, S.; Medvedik, O.; Sinclair, D. A.; Olefsky, J. M.; Jirousek, M. R.; Elliott, P. J.; Westphal, C. H.,

Small molecule activators of SIRT1 as therapeutics for the treatment of type 2 diabetes. *Nature* **2007,** *450* (7170), 712-6.
[35] Feige, J. N.; Lagouge, M.; Canto, C.; Strehle, A.; Houten, S. M.; Milne, J. C.; Lambert, P. D.; Mataki, C.; Elliott, P. J.; Auwerx, J., Specific SIRT1 activation mimics low energy levels and protects against diet-induced metabolic disorders by enhancing fat oxidation. *Cell Metab* **2008,** *8* (5), 347-58.
[36] Rodgers, J. T.; Lerin, C.; Haas, W.; Gygi, S. P.; Spiegelman, B. M.; Puigserver, P., Nutrient control of glucose homeostasis through a complex of PGC-1alpha and SIRT1. *Nature* **2005,** *434* (7029), 113-8.
[37] Purushotham, A.; Schug, T. T.; Xu, Q.; Surapureddi, S.; Guo, X.; Li, X., Hepatocyte-specific deletion of SIRT1 alters fatty acid metabolism and results in hepatic steatosis and inflammation. *Cell Metab* **2009,** *9* (4), 327-38.
[38] Walker, A. K.; Yang, F.; Jiang, K.; Ji, J. Y.; Watts, J. L.; Purushotham, A.; Boss, O.; Hirsch, M. L.; Ribich, S.; Smith, J. J.; Israelian, K.; Westphal, C. H.; Rodgers, J. T.; Shioda, T.; Elson, S. L.; Mulligan, P.; Najafi-Shoushtari, H.; Black, J. C.; Thakur, J. K.; Kadyk, L. C.; Whetstine, J. R.; Mostoslavsky, R.; Puigserver, P.; Li, X.; Dyson, N. J.; Hart, A. C.; Naar, A. M., Conserved role of SIRT1 orthologs in fasting-dependent inhibition of the lipid/cholesterol regulator SREBP. *Genes Dev* **2010,** *24* (13), 1403-17.
[39] Jiang, W.; Wang, S.; Xiao, M.; Lin, Y.; Zhou, L.; Lei, Q.; Xiong, Y.; Guan, K. L.; Zhao, S., Acetylation regulates gluconeogenesis by promoting PEPCK1 degradation via recruiting the UBR5 ubiquitin ligase. *Mol Cell* **2011,** *43* (1), 33-44.
[40] Hallows, W. C.; Lee, S.; Denu, J. M., Sirtuins deacetylate and activate mammalian acetyl-CoA synthetases. *Proc Natl Acad Sci U S A* **2006,** *103* (27), 10230-5.
[41] Hirschey, M. D.; Shimazu, T.; Goetzman, E.; Jing, E.; Schwer, B.; Lombard, D. B.; Grueter, C. A.; Harris, C.; Biddinger, S.; Ilkayeva, O. R.; Stevens, R. D.; Li, Y.; Saha, A. K.; Ruderman, N. B.; Bain, J. R.; Newgard, C. B.; Farese, R. V., Jr.; Alt, F. W.; Kahn, C. R.; Verdin, E., SIRT3 regulates mitochondrial fatty-acid oxidation by reversible enzyme deacetylation. *Nature* **2010,** *464* (7285), 121-5.
[42] Hallows, W. C.; Yu, W.; Smith, B. C.; Devries, M. K.; Ellinger, J. J.; Someya, S.; Shortreed, M. R.; Prolla, T.; Markley, J. L.; Smith, L. M.; Zhao, S.; Guan, K. L.; Denu, J. M., Sirt3 promotes the urea cycle and fatty acid oxidation during dietary restriction. *Mol Cell* **2011,** *41* (2), 139-49.
[43] Haigis, M. C.; Mostoslavsky, R.; Haigis, K. M.; Fahie, K.; Christodoulou, D. C.; Murphy, A. J.; Valenzuela, D. M.; Yancopoulos, G. D.; Karow, M.; Blander, G.; Wolberger, C.; Prolla, T. A.; Weindruch, R.; Alt, F. W.; Guarente, L., SIRT4 inhibits glutamate dehydrogenase and opposes the effects of calorie restriction in pancreatic beta cells. *Cell* **2006,** *126* (5), 941-54.
[44] Nasrin, N.; Wu, X.; Fortier, E.; Feng, Y.; Bare, O. C.; Chen, S.; Ren, X.; Wu, Z.; Streeper, R. S.; Bordone, L., SIRT4 regulates fatty acid oxidation and mitochondrial gene expression in liver and muscle cells. *J Biol Chem* **2010,** *285* (42), 31995-2002.
[45] Ahuja, N.; Schwer, B.; Carobbio, S.; Waltregny, D.; North, B. J.; Castronovo, V.; Maechler, P.; Verdin, E., Regulation of insulin secretion by SIRT4, a mitochondrial ADP-ribosyltransferase. *J Biol Chem* **2007,** *282* (46), 33583-92.
[46] Nakagawa, T.; Lomb, D. J.; Haigis, M. C.; Guarente, L., SIRT5 Deacetylates carbamoyl phosphate synthetase 1 and regulates the urea cycle. *Cell* **2009,** *137* (3), 560-70.
[47] Deng, C. X., SIRT1, is it a tumor promoter or tumor suppressor? *Int J Biol Sci* **2009,** *5* (2), 147-52.

[48] Hu, J.; Jing, H.; Lin, H., Sirtuin inhibitors as anticancer agents. *Future Med Chem* **2014,** *6* (8), 945-66.
[49] Chen, X.; Sun, K.; Jiao, S.; Cai, N.; Zhao, X.; Zou, H.; Xie, Y.; Wang, Z.; Zhong, M.; Wei, L., High levels of SIRT1 expression enhance tumorigenesis and associate with a poor prognosis of colorectal carcinoma patients. *Sci Rep* **2014,** *4*, 7481.
[50] Huffman, D. M.; Grizzle, W. E.; Bamman, M. M.; Kim, J. S.; Eltoum, I. A.; Elgavish, A.; Nagy, T. R., SIRT1 is significantly elevated in mouse and human prostate cancer. *Cancer Res* **2007,** *67* (14), 6612-8.
[51] Holloway, K. R.; Barbieri, A.; Malyarchuk, S.; Saxena, M.; Nedeljkovic-Kurepa, A.; Cameron Mehl, M.; Wang, A.; Gu, X.; Pruitt, K., SIRT1 positively regulates breast cancer associated human aromatase (CYP19A1) expression. *Mol Endocrinol* **2013,** *27* (3), 480-90.
[52] Bradbury, C. A.; Khanim, F. L.; Hayden, R.; Bunce, C. M.; White, D. A.; Drayson, M. T.; Craddock, C.; Turner, B. M., Histone deacetylases in acute myeloid leukaemia show a distinctive pattern of expression that changes selectively in response to deacetylase inhibitors. *Leukemia* **2005,** *19* (10), 1751-9.
[53] Cea, M.; Soncini, D.; Fruscione, F.; Raffaghello, L.; Garuti, A.; Emionite, L.; Moran, E.; Magnone, M.; Zoppoli, G.; Reverberi, D.; Caffa, I.; Salis, A.; Cagnetta, A.; Bergamaschi, M.; Casciaro, S.; Pierri, I.; Damonte, G.; Ansaldi, F.; Gobbi, M.; Pistoia, V.; Ballestrero, A.; Patrone, F.; Bruzzone, S.; Nencioni, A., Synergistic interactions between HDAC and sirtuin inhibitors in human leukemia cells. *PLoS One* **2011,** *6* (7), e22739.
[54] Yeung, F.; Hoberg, J. E.; Ramsey, C. S.; Keller, M. D.; Jones, D. R.; Frye, R. A.; Mayo, M. W., Modulation of NF-kappaB-dependent transcription and cell survival by the SIRT1 deacetylase. *EMBO J* **2004,** *23* (12), 2369-80.
[55] Firestein, R.; Blander, G.; Michan, S.; Oberdoerffer, P.; Ogino, S.; Campbell, J.; Bhimavarapu, A.; Luikenhuis, S.; de Cabo, R.; Fuchs, C.; Hahn, W. C.; Guarente, L. P.; Sinclair, D. A., The SIRT1 deacetylase suppresses intestinal tumorigenesis and colon cancer growth. *PLoS One* **2008,** *3* (4), e2020.
[56] Kuo, S. J.; Lin, H. Y.; Chien, S. Y.; Chen, D. R., SIRT1 suppresses breast cancer growth through downregulation of the Bcl-2 protein. *Oncol Rep* **2013,** *30* (1), 125-30.
[57] Herranz, D.; Munoz-Martin, M.; Canamero, M.; Mulero, F.; Martinez-Pastor, B.; Fernandez-Capetillo, O.; Serrano, M., Sirt1 improves healthy ageing and protects from metabolic syndrome-associated cancer. *Nat Commun* **2010,** *1*, 3.
[58] Wang, R. H.; Sengupta, K.; Li, C.; Kim, H. S.; Cao, L.; Xiao, C.; Kim, S.; Xu, X.; Zheng, Y.; Chilton, B.; Jia, R.; Zheng, Z. M.; Appella, E.; Wang, X. W.; Ried, T.; Deng, C. X., Impaired DNA damage response, genome instability, and tumorigenesis in SIRT1 mutant mice. *Cancer Cell* **2008,** *14* (4), 312-23.
[59] Hiratsuka, M.; Inoue, T.; Toda, T.; Kimura, N.; Shirayoshi, Y.; Kamitani, H.; Watanabe, T.; Ohama, E.; Tahimic, C. G.; Kurimasa, A.; Oshimura, M., Proteomics-based identification of differentially expressed genes in human gliomas: down-regulation of SIRT2 gene. *Biochem Biophys Res Commun* **2003,** *309* (3), 558-66.
[60] Inoue, T.; Hiratsuka, M.; Osaki, M.; Yamada, H.; Kishimoto, I.; Yamaguchi, S.; Nakano, S.; Katoh, M.; Ito, H.; Oshimura, M., SIRT2, a tubulin deacetylase, acts to block the entry to chromosome condensation in response to mitotic stress. *Oncogene* **2007,** *26* (7), 945-57.
[61] Li, Z.; Xie, Q. R.; Chen, Z.; Lu, S.; Xia, W., Regulation of SIRT2 levels for human non-small cell lung cancer therapy. *Lung Cancer* **2013,** *82* (1), 9-15.

[62] Grozinger, C. M.; Chao, E. D.; Blackwell, H. E.; Moazed, D.; Schreiber, S. L., Identification of a class of small molecule inhibitors of the sirtuin family of NAD-dependent deacetylases by phenotypic screening. *J Biol Chem* **2001,** *276* (42), 38837-43.
[63] Wang, J.; Kim, T. H.; Ahn, M. Y.; Lee, J.; Jung, J. H.; Choi, W. S.; Lee, B. M.; Yoon, K. S.; Yoon, S.; Kim, H. S., Sirtinol, a class III HDAC inhibitor, induces apoptotic and autophagic cell death in MCF-7 human breast cancer cells. *Int J Oncol* **2012,** *41* (3), 1101-9.
[64] Alhazzazi, T. Y.; Kamarajan, P.; Joo, N.; Huang, J. Y.; Verdin, E.; D'Silva, N. J.; Kapila, Y. L., Sirtuin-3 (SIRT3), a novel potential therapeutic target for oral cancer. *Cancer* **2011,** *117* (8), 1670-8.
[65] Ota, H.; Tokunaga, E.; Chang, K.; Hikasa, M.; Iijima, K.; Eto, M.; Kozaki, K.; Akishita, M.; Ouchi, Y.; Kaneki, M., Sirt1 inhibitor, Sirtinol, induces senescence-like growth arrest with attenuated Ras-MAPK signaling in human cancer cells. *Oncogene* **2006,** *25* (2), 176-85.
[66] Wang, T. T.; Schoene, N. W.; Kim, E. K.; Kim, Y. S., Pleiotropic effects of the sirtuin inhibitor sirtinol involves concentration-dependent modulation of multiple nuclear receptor-mediated pathways in androgen-responsive prostate cancer cell LNCaP. *Mol Carcinog* **2013,** *52* (9), 676-85.
[67] Heltweg, B.; Gatbonton, T.; Schuler, A. D.; Posakony, J.; Li, H.; Goehle, S.; Kollipara, R.; Depinho, R. A.; Gu, Y.; Simon, J. A.; Bedalov, A., Antitumor activity of a small-molecule inhibitor of human silent information regulator 2 enzymes. *Cancer Res* **2006,** *66* (8), 4368-77.
[68] Zhang, Y.; Au, Q.; Zhang, M.; Barber, J. R.; Ng, S. C.; Zhang, B., Identification of a small molecule SIRT2 inhibitor with selective tumor cytotoxicity. *Biochem Biophys Res Commun* **2009,** *386* (4), 729-33.
[69] Kim, H. S.; Patel, K.; Muldoon-Jacobs, K.; Bisht, K. S.; Aykin-Burns, N.; Pennington, J. D.; van der Meer, R.; Nguyen, P.; Savage, J.; Owens, K. M.; Vassilopoulos, A.; Ozden, O.; Park, S. H.; Singh, K. K.; Abdulkadir, S. A.; Spitz, D. R.; Deng, C. X.; Gius, D., SIRT3 is a mitochondria-localized tumor suppressor required for maintenance of mitochondrial integrity and metabolism during stress. *Cancer Cell* **2010,** *17* (1), 41-52.
[70] Csibi, A.; Fendt, S. M.; Li, C.; Poulogiannis, G.; Choo, A. Y.; Chapski, D. J.; Jeong, S. M.; Dempsey, J. M.; Parkhitko, A.; Morrison, T.; Henske, E. P.; Haigis, M. C.; Cantley, L. C.; Stephanopoulos, G.; Yu, J.; Blenis, J., The mTORC1 pathway stimulates glutamine metabolism and cell proliferation by repressing SIRT4. *Cell* **2013,** *153* (4), 840-54.
[71] Sebastian, C.; Zwaans, B. M.; Silberman, D. M.; Gymrek, M.; Goren, A.; Zhong, L.; Ram, O.; Truelove, J.; Guimaraes, A. R.; Toiber, D.; Cosentino, C.; Greenson, J. K.; MacDonald, A. I.; McGlynn, L.; Maxwell, F.; Edwards, J.; Giacosa, S.; Guccione, E.; Weissleder, R.; Bernstein, B. E.; Regev, A.; Shiels, P. G.; Lombard, D. B.; Mostoslavsky, R., The histone deacetylase SIRT6 is a tumor suppressor that controls cancer metabolism. *Cell* **2012,** *151* (6), 1185-99.
[72] Ford, E.; Voit, R.; Liszt, G.; Magin, C.; Grummt, I.; Guarente, L., Mammalian Sir2 homolog SIRT7 is an activator of RNA polymerase I transcription. *Genes Dev* **2006,** *20* (9), 1075-80.
[73] Barber, M. F.; Michishita-Kioi, E.; Xi, Y.; Tasselli, L.; Kioi, M.; Moqtaderi, Z.; Tennen, R. I.; Paredes, S.; Young, N. L.; Chen, K.; Struhl, K.; Garcia, B. A.; Gozani, O.; Li, W.; Chua, K. F., SIRT7 links H3K18 deacetylation to maintenance of oncogenic transformation. *Nature* **2012,** *487* (7405), 114-8.

[74] Araki, T.; Sasaki, Y.; Milbrandt, J., Increased nuclear NAD biosynthesis and SIRT1 activation prevent axonal degeneration. *Science* **2004,** *305* (5686), 1010-3.
[75] Brunet, A.; Sweeney, L. B.; Sturgill, J. F.; Chua, K. F.; Greer, P. L.; Lin, Y.; Tran, H.; Ross, S. E.; Mostoslavsky, R.; Cohen, H. Y.; Hu, L. S.; Cheng, H. L.; Jedrychowski, M. P.; Gygi, S. P.; Sinclair, D. A.; Alt, F. W.; Greenberg, M. E., Stress-dependent regulation of FOXO transcription factors by the SIRT1 deacetylase. *Science* **2004,** *303* (5666), 2011-5.
[76] Kim, D.; Nguyen, M. D.; Dobbin, M. M.; Fischer, A.; Sananbenesi, F.; Rodgers, J. T.; Delalle, I.; Baur, J. A.; Sui, G.; Armour, S. M.; Puigserver, P.; Sinclair, D. A.; Tsai, L. H., SIRT1 deacetylase protects against neurodegeneration in models for Alzheimer's disease and amyotrophic lateral sclerosis. *EMBO J* **2007,** *26* (13), 3169-79.
[77] Patrick, G. N.; Zukerberg, L.; Nikolic, M.; de la Monte, S.; Dikkes, P.; Tsai, L. H., Conversion of p35 to p25 deregulates Cdk5 activity and promotes neurodegeneration. *Nature* **1999,** *402* (6762), 615-22.
[78] Outeiro, T. F.; Kontopoulos, E.; Altmann, S. M.; Kufareva, I.; Strathearn, K. E.; Amore, A. M.; Volk, C. B.; Maxwell, M. M.; Rochet, J. C.; McLean, P. J.; Young, A. B.; Abagyan, R.; Feany, M. B.; Hyman, B. T.; Kazantsev, A. G., Sirtuin 2 inhibitors rescue alpha-synuclein-mediated toxicity in models of Parkinson's disease. *Science* **2007,** *317* (5837), 516-9.
[79] Luthi-Carter, R.; Taylor, D. M.; Pallos, J.; Lambert, E.; Amore, A.; Parker, A.; Moffitt, H.; Smith, D. L.; Runne, H.; Gokce, O.; Kuhn, A.; Xiang, Z.; Maxwell, M. M.; Reeves, S. A.; Bates, G. P.; Neri, C.; Thompson, L. M.; Marsh, J. L.; Kazantsev, A. G., SIRT2 inhibition achieves neuroprotection by decreasing sterol biosynthesis. *Proc Natl Acad Sci U S A* **2010,** *107* (17), 7927-32.
[80] Pfister, J. A.; Ma, C.; Morrison, B. E.; D'Mello, S. R., Opposing effects of sirtuins on neuronal survival: SIRT1-mediated neuroprotection is independent of its deacetylase activity. *PLoS One* **2008,** *3* (12), e4090.
[81] Berman, H. M.; Westbrook, J.; Feng, Z.; Gilliland, G.; Bhat, T. N.; Weissig, H.; Shindyalov, I. N.; Bourne, P. E., The Protein Data Bank. *Nucleic Acids Research* **2000,** *28* (1), 235-242.
[82] http://www.rcsb.org/pdb/statistics/holdings.do.
[83] http://www.uniprot.org/.
[84] http://web.expasy.org/docs/relnotes/relstat.html.
[85] Cavasotto, C. N.; Phatak, S. S., Homology modeling in drug discovery: current trends and applications. *Drug Discov Today* **2009,** *14* (13-14), 676-83.
[86] Marti-Renom, M. A.; Stuart, A. C.; Fiser, A.; Sanchez, R.; Melo, F.; Sali, A., Comparative protein structure modeling of genes and genomes. *Annu Rev Biophys Biomol Struct* **2000,** *29*, 291-325.
[87] Kohler, J.; Erlenkamp, G.; Eberlin, A.; Rumpf, T.; Slynko, I.; Metzger, E.; Schule, R.; Sippl, W.; Jung, M., Lestaurtinib inhibits histone phosphorylation and androgen-dependent gene expression in prostate cancer cells. *PLoS One* **2012,** *7* (4), e34973.
[88] Pearson, W. R., Empirical statistical estimates for sequence similarity searches. *J Mol Biol* **1998,** *276* (1), 71-84.
[89] Altschul, S. F.; Gish, W.; Miller, W.; Myers, E. W.; Lipman, D. J., Basic local alignment search tool. *J Mol Biol* **1990,** *215* (3), 403-10.
[90] Jeanmougin, F.; Thompson, J. D.; Gouy, M.; Higgins, D. G.; Gibson, T. J., Multiple sequence alignment with Clustal X. *Trends Biochem Sci* **1998,** *23* (10), 403-5.

[91] Blundell, T.; Carney, D.; Gardner, S.; Hayes, F.; Howlin, B.; Hubbard, T.; Overington, J.; Singh, D. A.; Sibanda, B. L.; Sutcliffe, M., 18th Sir Hans Krebs lecture. Knowledge-based protein modelling and design. *Eur J Biochem* **1988,** *172* (3), 513-20.
[92] Sutcliffe, M. J.; Haneef, I.; Carney, D.; Blundell, T. L., Knowledge based modelling of homologous proteins, Part I: Three-dimensional frameworks derived from the simultaneous superposition of multiple structures. *Protein Eng* **1987,** *1* (5), 377-84.
[93] Sali, A.; Blundell, T. L., Comparative protein modelling by satisfaction of spatial restraints. *J Mol Biol* **1993,** *234* (3), 779-815.
[94] Laskowski, R. A.; MacArthur, M. W.; Moss, D. S.; Thornton, J. M., PROCHECK: a program to check the stereochemical quality of protein structures. . *J Appl Crystallogr* **1993,** *26*, 283-291.
[95]http://blast.ncbi.nlm.nih.gov/Blast.cgi?PROGRAM=blastp&PAGE_TYPE=BlastSearch&LINK_LOC=blasthome.
[96] *Molecular Operating Environment (MOE); 2012.10, Chemical Computing Group Inc.: Montreal, Canada. 2012.*
[97] Shen, M. Y.; Sali, A., Statistical potential for assessment and prediction of protein structures. *Protein Sci* **2006,** *15* (11), 2507-24.
[98] Wereszczynski, J.; McCammon, J. A., Statistical mechanics and molecular dynamics in evaluating thermodynamic properties of biomolecular recognition. *Q Rev Biophys* **2012,** *45* (1), 1-25.
[99] Bishop, A. O. T.; Beer, T. A. P. d.; Joubert, F., Protein homology modelling and its use in South Africa. *S. Afr. j. sci.* **2008,** *104* (1-2), 2-6.
[100] Yuriev, E.; Agostino, M.; Ramsland, P. A., Challenges and advances in computational docking: 2009 in review. *J Mol Recognit* **2011,** *24* (2), 149-64.
[101] Warren, G. L.; Andrews, C. W.; Capelli, A. M.; Clarke, B.; LaLonde, J.; Lambert, M. H.; Lindvall, M.; Nevins, N.; Semus, S. F.; Senger, S.; Tedesco, G.; Wall, I. D.; Woolven, J. M.; Peishoff, C. E.; Head, M. S., A critical assessment of docking programs and scoring functions. *J Med Chem* **2006,** *49* (20), 5912-31.
[102] Moitessier, N.; Englebienne, P.; Lee, D.; Lawandi, J.; Corbeil, C. R., Towards the development of universal, fast and highly accurate docking/scoring methods: a long way to go. *Br J Pharmacol* **2008,** *153 Suppl 1*, S7-26.
[103] Vaque, M. A., Anna; Blade, Cinta; Salvado, M. J.; Blay, Mayte; Fernandez-Larrea, Juan; Arola, Lluis, Pujadas, Gerard, Protein-ligand Docking: A Review of Recent Advances and Future Perspectives. *Current Pharmaceutical Analysis* **2008,** *4*, 1-19.
[104] LigPrep, version 2.5, Schrödinger, LLC, New York, NY. 2011.
[105] Sherman, W.; Day, T.; Jacobson, M. P.; Friesner, R. A.; Farid, R., Novel procedure for modeling ligand/receptor induced fit effects. *J Med Chem* **2006,** *49* (2), 534-53.
[106] Höltje, H.-D.; Sippl, W.; Rognan, D.; Folkers, G., Scope and Limits of Molecular Docking. In *Molecular Modeling*, Third, Revised and Expanded Edition ed.; Wiley-VCH Verlag GmbH: 2008; pp 217-231.
[107] Labute, P., Protonate3D: assignment of ionization states and hydrogen coordinates to macromolecular structures. *Proteins* **2009,** *75* (1), 187-205.
[108] Wang, J.; Cieplak, P.; Kollman, P. A., How well does a restrained electrostatic potential (RESP) model perform in calculating conformational energies of organic and biological molecules? *J Comput Chem* **2000,** *21* (12), 1049-1074.
[109] Jones, G.; Willett, P.; Glen, R. C., Molecular recognition of receptor sites using a genetic algorithm with a description of desolvation. *J Mol Biol* **1995,** *245* (1), 43-53.

[110] Jones, G.; Willett, P.; Glen, R. C.; Leach, A. R.; Taylor, R., Development and validation of a genetic algorithm for flexible docking. *J Mol Biol* **1997,** *267* (3), 727-48.
[111] Nissink, J. W. M.; Murray, C.; Hartshorn, M.; Verdonk, M. L.; Cole, J. C.; Taylor, R., A new test set for validating predictions of protein–ligand interaction. *Proteins: Structure, Function, and Bioinformatics* **2002,** *49* (4), 457-471.
[112] Verdonk, M. L.; Cole, J. C.; Hartshorn, M. J.; Murray, C. W.; Taylor, R. D., Improved protein–ligand docking using GOLD. *Proteins: Structure, Function, and Bioinformatics* **2003,** *52* (4), 609-623.
[113] Hartshorn, M. J.; Verdonk, M. L.; Chessari, G.; Brewerton, S. C.; Mooij, W. T. M.; Mortenson, P. N.; Murray, C. W., Diverse, High-Quality Test Set for the Validation of Protein−Ligand Docking Performance. *J Med Chem* **2007,** *50* (4), 726-741.
[114] Glide, Version 5.8; Schrödinger, LLC: New York, 2012.
[115] Halgren, T. A.; Murphy, R. B.; Friesner, R. A.; Beard, H. S.; Frye, L. L.; Pollard, W. T.; Banks, J. L., Glide: A New Approach for Rapid, Accurate Docking and Scoring. 2. Enrichment Factors in Database Screening. *J Med Chem* **2004,** *47* (7), 1750-1759.
[116] Friesner, R. A.; Murphy, R. B.; Repasky, M. P.; Frye, L. L.; Greenwood, J. R.; Halgren, T. A.; Sanschagrin, P. C.; Mainz, D. T., Extra Precision Glide: Docking and Scoring Incorporating a Model of Hydrophobic Enclosure for Protein−Ligand Complexes. *J Med Chem* **2006,** *49* (21), 6177-6196.
[117] Friesner, R. A.; Banks, J. L.; Murphy, R. B.; Halgren, T. A.; Klicic, J. J.; Mainz, D. T.; Repasky, M. P.; Knoll, E. H.; Shelley, M.; Perry, J. K.; Shaw, D. E.; Francis, P.; Shenkin, P. S., Glide: A New Approach for Rapid, Accurate Docking and Scoring. 1. Method and Assessment of Docking Accuracy. *J Med Chem* **2004,** *47* (7), 1739-1749.
[118] Verdonk, M. L.; Chessari, G.; Cole, J. C.; Hartshorn, M. J.; Murray, C. W.; Nissink, J. W. M.; Taylor, R. D.; Taylor, R., Modeling Water Molecules in Protein−Ligand Docking Using GOLD. *J Med Chem* **2005,** *48* (20), 6504-6515.
[119] http://www.lhasalimited.org/products/derek-nexus.htm.
[120] Sanderson, D. M.; Earnshaw, C. G., Computer prediction of possible toxic action from chemical structure; the DEREK system. *Hum Exp Toxicol* **1991,** *10* (4), 261-73.
[121] Ridings, J. E.; Barratt, M. D.; Cary, R.; Earnshaw, C. G.; Eggington, C. E.; Ellis, M. K.; Judson, P. N.; Langowski, J. J.; Marchant, C. A.; Payne, M. P.; Watson, W. P.; Yih, T. D., Computer prediction of possible toxic action from chemical structure: an update on the DEREK system. *Toxicology* **1996,** *106* (1-3), 267-79.
[122] Greene, N.; Judson, P. N.; Langowski, J. J.; Marchant, C. A., Knowledge-based expert systems for toxicity and metabolism prediction: DEREK, StAR and METEOR. *SAR QSAR Environ Res* **1999,** *10* (2-3), 299-314.
[123] Marchant, C. A.; Briggs, K. A.; Long, A., In silico tools for sharing data and knowledge on toxicity and metabolism: derek for windows, meteor, and vitic. *Toxicol Mech Methods* **2008,** *18* (2-3), 177-87.
[124] Lin, J. H.; Lu, A. Y., Role of pharmacokinetics and metabolism in drug discovery and development. *Pharmacol Rev* **1997,** *49* (4), 403-49.
[125] QikProp, version 3.4, Schrödinger, LLC, New York, NY, 2011.
[126] Lipinski, C. A.; Lombardo, F.; Dominy, B. W.; Feeney, P. J., Experimental and computational approaches to estimate solubility and permeability in drug discovery and development settings. *Adv Drug Deliv Rev* **2001,** *46* (1-3), 3-26.
[127] Bajorath, J., Integration of virtual and high-throughput screening. *Nat Rev Drug Discov* **2002,** *1* (11), 882-94.

[128] Cheng, T.; Li, Q.; Zhou, Z.; Wang, Y.; Bryant, S. H., Structure-based virtual screening for drug discovery: a problem-centric review. *AAPS J* **2012,** *14* (1), 133-41.
[129] Cole, J. C.; Korb, O.; Olsson, T. S. G.; Liebeschuetz, J., The Basis for Target-Based Virtual Screening: Protein Structures. In *Virtual Screening*, Wiley-VCH Verlag GmbH & Co. KGaA: 2011; pp 87-114.
[130] Verdonk, M. L.; Berdini, V.; Hartshorn, M. J.; Mooij, W. T.; Murray, C. W.; Taylor, R. D.; Watson, P., Virtual screening using protein-ligand docking: avoiding artificial enrichment. *J Chem Inf Comput Sci* **2004,** *44* (3), 793-806.
[131] Chen, Y. C., Beware of docking! *Trends Pharmacol Sci* **2015,** *36* (2), 78-95.
[132] Halgren, T. A., Merck molecular force field. I. Basis, form, scope, parameterization, and performance of MMFF94. *J Comput Chem* **1996,** *17* (5-6), 490-519.
[133] Halgren, T. A., Merck molecular force field. II. MMFF94 van der Waals and electrostatic parameters for intermolecular interactions. *J Comput Chem* **1996,** *17* (5-6), 520-552.
[134] Halgren, T. A., Merck molecular force field. III. Molecular geometries and vibrational frequencies for MMFF94. *J Comput Chem* **1996,** *17* (5-6), 553-586.
[135] Halgren, T. A.; Nachbar, R. B., Merck molecular force field. IV. conformational energies and geometries for MMFF94. *J Comput Chem* **1996,** *17* (5-6), 587-615.
[136] Halgren, T. A., Merck molecular force field. V. Extension of MMFF94 using experimental data, additional computational data, and empirical rules. *J Comput Chem* **1996,** *17* (5-6), 616-641.
[137] Maestro, version 9.3, 2012.
[138] Wermuth, C. G.; Ganellin, C. R.; Lindberg, P.; Mitscher, L. A., Glossary of terms used in Medicinal Chemistry (IUPAC Recommendations 1998) *Pure & Appl. Chem.* **1998,** *70*, 1129-1143.
[139] Koeppen, H.; Kriegl, J.; Lessel, U.; Tautermann, C. S.; Wellenzohn, B., Ligand-Based Virtual Screening. In *Virtual Screening*, Wiley-VCH Verlag GmbH & Co. KGaA: 2011; pp 61-85.
[140] Markt, P.; Schuster, D.; Langer, T., Pharmacophore Models for Virtual Screening. In *Virtual Screening*, Wiley-VCH Verlag GmbH & Co. KGaA: 2011; pp 115-152.
[141] Wolber, G.; Langer, T., LigandScout: 3-D pharmacophores derived from protein-bound ligands and their use as virtual screening filters. *J Chem Inf Model* **2005,** *45* (1), 160-9.
[142] http://dude.docking.org/.
[143] Mysinger, M. M.; Carchia, M.; Irwin, J. J.; Shoichet, B. K., Directory of Useful Decoys, Enhanced (DUD-E): Better Ligands and Decoys for Better Benchmarking. *J Med Chem* **2012,** *55* (14), 6582-6594.
[144] Huang, N.; Shoichet, B. K.; Irwin, J. J., Benchmarking Sets for Molecular Docking. *J Med Chem* **2006,** *49* (23), 6789-6801.
[145] Durrant, J. D.; McCammon, J. A., Molecular dynamics simulations and drug discovery. *BMC Biol* **2011,** *9*, 71.
[146] Case, D. A. D., T. A.; Cheatham, III, T. E.; Simmerling, C.; L.; Wang, J. D., R. E.; Luo, R.; Walker, R. C.; Zhang, W.; Merz, K.; M.; et al.; et al. AMBER 12; University of California, S. F., 2012.
[147] Duan, Y.; Wu, C.; Chowdhury, S.; Lee, M. C.; Xiong, G.; Zhang, W.; Yang, R.; Cieplak, P.; Luo, R.; Lee, T.; Caldwell, J.; Wang, J.; Kollman, P., A point-charge force field for molecular mechanics simulations of proteins based on condensed-phase quantum mechanical calculations. *J Comput Chem* **2003,** *24* (16), 1999-2012.

[148] Jakalian, A.; Jack, D. B.; Bayly, C. I., Fast, efficient generation of high-quality atomic charges. AM1-BCC model: II. Parameterization and validation. *J Comput Chem* **2002,** *23* (16), 1623-41.
[149] Wang, J.; Wolf, R. M.; Caldwell, J. W.; Kollman, P. A.; Case, D. A., Development and testing of a general amber force field. *J Comput Chem* **2004,** *25* (9), 1157-74.
[150] zinc library page. http://www.mayo.edu/research/labs/computer-aided-molecular-design/projects/zinc-protein-simulations-using-cationic-dummy-atom-cada-approach.
[151] Jorgensen, W. L.; Chandrasekhar, J.; Madura, J. D.; Impey, R. W.; Klein, M. L., Comparison of simple potential functions for simulating liquid water. *The Journal of chemical physics* **1983,** *79* (2), 926-935.
[152] Pastor, R. W.; Brooks, B. R.; Szabo, A., An analysis of the accuracy of Langevin and molecular dynamics algorithms. *Molecular Physics* **1988,** *65* (6), 1409-1419.
[153] Darden, T.; York, D.; Pedersen, L., Particle mesh Ewald: An N·log(N) method for Ewald sums in large systems. *The Journal of chemical physics* **1993,** *98* (12), 10089-10092.
[154] Ryckaert, J.-P.; Ciccotti, G.; Berendsen, H. J. C., Numerical integration of the cartesian equations of motion of a system with constraints: molecular dynamics of n-alkanes. *Journal of Computational Physics* **1977,** *23* (3), 327-341.
[155] Gilson, M. K.; Zhou, H. X., Calculation of protein-ligand binding affinities. *Annu Rev Biophys Biomol Struct* **2007,** *36*, 21-42.
[156] Kirkwood, J. G., Statistical Mechanics of Fluid Mixtures. *The Journal of Chemical Physics* **1935,** *3* (5), 300-313.
[157] Straatsma, T. P.; McCammon, J. A., Multiconfiguration thermodynamic integration. *The Journal of Chemical Physics* **1991,** *95* (2), 1175-1188.
[158] Aqvist, J.; Medina, C.; Samuelsson, J. E., A new method for predicting binding affinity in computer-aided drug design. *Protein Eng* **1994,** *7* (3), 385-91.
[159] Srinivasan, J.; Cheatham, T. E.; Cieplak, P.; Kollman, P. A.; Case, D. A., Continuum Solvent Studies of the Stability of DNA, RNA, and Phosphoramidate−DNA Helices. *J Am Chem Soc* **1998,** *120* (37), 9401-9409.
[160] Kuhn, B.; Gerber, P.; Schulz-Gasch, T.; Stahl, M., Validation and use of the MM-PBSA approach for drug discovery. *J Med Chem* **2005,** *48* (12), 4040-8.
[161] Rastelli, G.; Del Rio, A.; Degliesposti, G.; Sgobba, M., Fast and accurate predictions of binding free energies using MM-PBSA and MM-GBSA. *J Comput Chem* **2010,** *31* (4), 797-810.
[162] Wichapong, K.; Lawson, M.; Pianwanit, S.; Kokpol, S.; Sippl, W., Postprocessing of protein-ligand docking poses using linear response MM-PB/SA: application to Wee1 kinase inhibitors. *J Chem Inf Model* **2010,** *50* (9), 1574-88.
[163] Lindstrom, A.; Edvinsson, L.; Johansson, A.; Andersson, C. D.; Andersson, I. E.; Raubacher, F.; Linusson, A., Postprocessing of docked protein-ligand complexes using implicit solvation models. *J Chem Inf Model* **2011,** *51* (2), 267-82.
[164] Slynko, I.; Scharfe, M.; Rumpf, T.; Eib, J.; Metzger, E.; Schule, R.; Jung, M.; Sippl, W., Virtual screening of PRK1 inhibitors: ensemble docking, rescoring using binding free energy calculation and QSAR model development. *J Chem Inf Model* **2014,** *54* (1), 138-50.
[165] Rastelli, G.; Degliesposti, G.; Del Rio, A.; Sgobba, M., Binding Estimation after Refinement, a New Automated Procedure for the Refinement and Rescoring of Docked Ligands in Virtual Screening. *Chemical Biology & Drug Design* **2009,** *73* (3), 283-286.
[166] Uciechowska, U.; Schemies, J.; Scharfe, M.; Lawson, M.; Wichapong, K.; Jung, M.; Sippl, W., Binding free energy calculations and biological testing of novel thiobarbiturates as

inhibitors of the human NAD(+) dependent histone deacetylase Sirt2. *Medchemcomm* **2012,** *3* (2), 167-173.
[167] Hawkins, G. D.; Cramer, C. J.; Truhlar, D. G., Pairwise Solute Descreening of Solute Charges from a Dielectric Medium. *Chem Phys Lett* **1995,** *246* (1-2), 122-129.
[168] Hawkins, G. D.; Cramer, C. J.; Truhlar, D. G., Parametrized models of aqueous free energies of solvation based on pairwise descreening of solute atomic charges from a dielectric medium. *J Phys Chem-Us* **1996,** *100* (51), 19824-19839.
[169] Tsui, V.; Case, D. A., Theory and applications of the generalized Born solvation model in macromolecular Simulations. *Biopolymers* **2001,** *56* (4), 275-291.
[170] Onufriev, A.; Bashford, D.; Case, D. A., Exploring protein native states and large-scale conformational changes with a modified generalized born model. *Proteins-Structure Function and Bioinformatics* **2004,** *55* (2), 383-394.
[171] Mongan, J.; Simmerling, C.; McCammon, J. A.; Case, D. A.; Onufriev, A., Generalized Born model with a simple, robust molecular volume correction. *J Chem Theory Comput* **2007,** *3* (1), 156-169.
[172] Homeyer, N.; Gohlke, H., Free Energy Calculations by the Molecular Mechanics Poisson−Boltzmann Surface Area Method. *Molecular Informatics* **2012,** *31* (2), 114-122.
[173] Hou, T.; Wang, J.; Li, Y.; Wang, W., Assessing the performance of the MM/PBSA and MM/GBSA methods. 1. The accuracy of binding free energy calculations based on molecular dynamics simulations. *J Chem Inf Model* **2011,** *51* (1), 69-82.
[174] Wang, R. X.; Lai, L. H.; Wang, S. M., Further development and validation of empirical scoring functions for structure-based binding affinity prediction. *J Comput Aid Mol Des* **2002,** *16* (1), 11-26.
[175] Giordanetto, F.; Cotesta, S.; Catana, C.; Trosset, J. Y.; Vulpetti, A.; Stouten, P. F. W.; Kroemer, R. T., Novel scoring functions comprising QXP, SASA, and protein side-chain entropy terms. *J Chem Inf Comp Sci* **2004,** *44* (3), 882-893.
[176] Raha, K.; Merz, K. M., A quantum mechanics-based scoring function: Study of zinc ion-mediated ligand binding. *J Am Chem Soc* **2004,** *126* (4), 1020-1021.
[177] Thompson, D. C.; Humblet, C.; Joseph-McCarthy, D., Investigation of MM-PBSA rescoring of docking poses. *J Chem Inf Model* **2008,** *48* (5), 1081-91.
[178] Wichapong, K.; Rohe, A.; Platzer, C.; Slynko, I.; Erdmann, F.; Schmidt, M.; Sippl, W., Application of docking and QM/MM-GBSA rescoring to screen for novel Myt1 kinase inhibitors. *J Chem Inf Model* **2014,** *54* (3), 881-93.
[179] Hayik, S. A.; Dunbrack, R.; Merz, K. M., Mixed Quantum Mechanics/Molecular Mechanics Scoring Function To Predict Protein−Ligand Binding Affinity. *J Chem Theory Comput* **2010,** *6* (10), 3079-3091.
[180] Karaman, B.; Sippl, W., Docking and binding free energy calculations of sirtuin inhibitors. *Eur J Med Chem* **2015,** *93*, 584-98.
[181] Rumpf, T.; Schiedel, M.; Karaman, B.; Roessler, C.; North, B. J.; Lehotzky, A.; Oláh, J.; Ladwein, K. I.; Schmidtkunz, K.; Gajer, M.; Pannek, M.; Steegborn, C.; Sinclair, D. A.; Gerhardt, S.; Ovádi, J.; Schutkowski, M.; Sippl, W.; Einsle, O.; Jung, M., Selective Sirt2 inhibition by ligand-induced rearrangement of the active site. *Nat Commun* **2015,** *6*.
[182] Velema, W. A.; Szymanski, W.; Feringa, B. L., Photopharmacology: Beyond Proof of Principle. *J Am Chem Soc* **2014,** *136* (6), 2178-2191.
[183] Falenczyk, C.; Schiedel, M.; Karaman, B.; Rumpf, T.; Kuzmanovic, N.; Grotli, M.; Sippl, W.; Jung, M.; Konig, B., Chromo-pharmacophores: photochromic diarylmaleimide inhibitors for sirtuins. *Chemical Science* **2014,** *5* (12), 4794-4799.

[184] Trapp, J.; Jochum, A.; Meier, R.; Saunders, L.; Marshall, B.; Kunick, C.; Verdin, E.; Goekjian, P.; Sippl, W.; Jung, M., Adenosine mimetics as inhibitors of NAD+-dependent histone deacetylases, from kinase to sirtuin inhibition. *J Med Chem* **2006,** *49* (25), 7307-16.
[185] http://www.who.int/mediacentre/factsheets/fs115/en/.
[186] Lancelot, J.; Caby, S.; Dubois-Abdesselem, F.; Vanderstraete, M.; Trolet, J.; Oliveira, G.; Bracher, F.; Jung, M.; Pierce, R. J., Schistosoma mansoni Sirtuins: characterization and potential as chemotherapeutic targets. *PLoS Negl Trop Dis* **2013,** *7* (9), e2428.
[187] Schiedel, M.; Marek, M.; Lancelot, J.; Karaman, B.; Almlof, I.; Schultz, J.; Sippl, W.; Pierce, R. J.; Romier, C.; Jung, M., Fluorescence-based screening assays for the NAD(+)-dependent histone deacetylase smSirt2 from Schistosoma mansoni. *J Biomol Screen* **2015,** *20* (1), 112-21.
[188] Newman, D. J.; Cragg, G. M., Natural Products As Sources of New Drugs over the 30 Years from 1981 to 2010. *J Nat Prod* **2012,** *75* (3), 311-335.
[189] Ntie-Kang, F.; Nwodo, J. N.; Ibezim, A.; Simoben, C. V.; Karaman, B.; Ngwa, V. F.; Sippl, W.; Adikwu, M. U.; Mbaze, L. M., Molecular modeling of potential anticancer agents from African medicinal plants. *J Chem Inf Model* **2014,** *54* (9), 2433-50.
[190] http://www.who.int/mediacentre/factsheets/fs297/en/.
[191] Newman, D. J.; Cragg, G. M., Natural products as sources of new drugs over the 30 years from 1981 to 2010. *J Nat Prod* **2012,** *75* (3), 311-35.
[192] Mangal, M.; Sagar, P.; Singh, H.; Raghava, G. P.; Agarwal, S. M., NPACT: Naturally Occurring Plant-based Anti-cancer Compound-Activity-Target database. *Nucleic Acids Res* **2013,** *41* (Database issue), D1124-9.
[193] Dictionary of Natural Products on CD-Rom; Chapman and Hall/CRC Press: London, 2005.

7. Appendix

Selbststandigkeitserklarung

Hiermit erkläre ich, dass ich die vorliegende Dissertationsschrift selbständig und ohne fremde Hilfe angefertigt, keine anderen als die angegebenen Quellen und Hilfsmittel benutzt und die aus ihnen wörtlich oder inhaltlich entnommenen Stellen als solche kenntlich gemacht habe.

Die Arbeit wurde ausschließlich der Mathematisch-Naturwissenschaftlichen Fakultät der Martin-Luther-Universität Halle-Wittenberg vorgelegt und an keiner anderen Universität oder Hochschule weder im In- und Ausland zur Erlangung des Doktorgrades eingereicht.

Halle (Saale), den 28.07.2015 M.Sc. Berin Karaman

Curriculum Vitae

Berin Karaman

Tel (Office): 0049-345-55-25043
Fax (Office): 0049-345-55-27355
e-mail: berin.karaman@pharmazie.uni-halle.de
karaman.berin@gmail.com
Profile: https://www.researchgate.net/profile/Berin_Karaman
www.linkedin.com (https://goo.gl/E4Tkif)
Address (Office): Martin-Luther-University Halle-Wittenberg, Institute of Pharmacy, Wolfgang-Langenbeck-Str.4, 06120, Halle (Saale), Germany

Education

2011 - 2015 **Martin-Luther-University Halle-Wittenberg, Germany**
Ph.D., Institute of Pharmacy, Research Group of Medicinal Chemistry

2008 - 2010 **Istanbul University**, **Turkey**
M.Sc., Institute of Pharmacy, Pharmaceutical Chemistry Department (GPA: 97.09/100)

2004 - 2008 **Marmara University, Turkey**
Bachelor Degree of Pharmacy, Salutatorian (GPA: 89.29/100)
Licensed Pharmacist in Turkey

Awards and Funds

2013 - current **EU-Project A-PARADDISE**
I am funded by EU-Project A-PARADDISE (Anti-Parasitic Drug Discovery in Epigenetics) for my graduate studies.

2013 **Best Poster Prize**
Innovative Approaches to Computational Drug Discovery Workshop, Lausanne.

2011 - 2013 **Landesgraduiertenförderung Sachsen-Anhalt Scholarship**
Scholarship for graduate studies in Ph.D. given by state, Sachsen-Anhalt, of Germany.

2008 - 2010 **TUBITAK National Scholarship**
Scholarship for graduate studies in M.Sc. given by TUBITAK (Turkish Scientific and Technical Research Council).

Research Experience

2011- current **Martin-Luther-University Halle-Wittenberg, Germany**
Ph.D. Research Assistant & Graduate Student with Prof. Wolfgang Sippl
Dissertation: Application of computer-based methods to guide the development of novel sirtuin inhibitors. Tested and applied various computational methods including docking, virtual screening, pharmacophore generation, homology modeling, molecular dynamics simulations, binding free energy calculations and development of QSAR models.

2008 - 2010 **Istanbul University, Turkey**
M.Sc. Graduate Student with Prof. Nuray Ulusoy Guzeldemirci
Thesis: Synthesis of imidazo[2,1-*b*]thiazole derivatives.

Summer 2007 **Marmara University, Turkey**
Fall 2008 Voluntary laboratory work
Synthesis of some novel hydrazide-hydrazones with Prof. S. Guniz Kucukgu
Pharmaceutical Chemistry Department

Teaching Experience

Fall 2015 **Martin-Luther-University Halle-Wittenberg, Germany**
Fall 2014 Supervisor of "Protein Modeling and Simulation Lab Course" (Master
Fall 2013 students) – taught and graded

2008 - 2010 **Istanbul University, Turkey**
Voluntary teaching assistant of Undergraduate Pharmaceutical Chemistry Labs – taught and graded
Pharmaceutical Chemistry-1 / Synthesis Lab.
Pharmaceutical Chemistry-2 **/** Qualitative Analysis Lab.
Pharmaceutical Chemistry-3 **/** Quantitative Analysis Lab.

Related Professional Experience

09/2010 - 03/2011 **Sisli Florence Nightingale Hospital, Pharmacy, Turkey**
Hospital Pharmacist, Supervisor; Figen Camci

Publications

➢ Book Chapter

Karaman, B.; Jung M.; Sippl, W. Structure-based design and computational studies of sirtuin inhibitors**.**
In: Epi-Informatics: Discovery and Development of Small Molecule Epigenetic Drugs and Probes Using Computational Approaches. Ed. Jose Medina-Franco, Elsevier, **2015 (accepted)**

➢ Journal Articles

I. Schiedel, M.; Rumpf, T.; **Karaman, B.;** Lehotzky, A.; Gerhardt, S.; Ovádi, J.; Sippl, W.; Einsle, O.; Jung, M. Aminothiazoles as potent and selective Sirt2 inhibitors – a structure-activity relationship study. **2015 (submitted)**

II. **Karaman, B**. and Nuray Ulusoy Güzeldemirci. Synthesis and biological evaluation of new imidazo[2,1-b]thiazole derivatives as anticancer agents. **2015 (submitted)**

III. Ntie-Kang, F.; Simoben C. V.; **Karaman, B.**; Ngwa, V. F.; Lifongo, L.L.; Judson, P. N.; Sippl, W.; Mbaze, L. C. Pharmacophore Modeling and in Silico Toxicity Assessment of Potential Anticancer Agents from African Medicinal Plants. **2015 (in review)**

IV. **Karaman, B.** and Sippl, W. Docking and binding free energy calculations of sirtuin inhibitors. **2015**
European Journal of Medicinal Chemistry, 5-Year Impact Factor: 4.071.

V. Rumpf, T.; Schiedel, M.; **Karaman, B**.; Rössler, C.; North, B. J.; Ladwein, K. I.; Gajer, M.; Sinclair, D. A.; Schutkowski, M.; Sippl, W.; Einsle, O.; Jung, M. Structural basis for selective inhibition of hSirt2 by ligand induced rearrangement of the active site. **2015**
Nature Communications, Impact Factor: 10.742.

VI. Falenczyk, C.; Schiedel, M.; **Karaman, B.**; Rumpf, T.; Kuzmanovic, N.; Grotli, M.; Sippl, W.; Jung, M.; Konig, B., Chromo-pharmacophores: photochromic diarylmaleimide inhibitors for sirtuins. **2014**.
Chemical Science - Royal Society of Chemistry, Impact Factor: 8.601.

VII. Schiedel, M.; Marek, M.; Lancelot, J.; **Karaman, B**.; Almlöf, I.; Schultz, J.; Sippl, W.; Pierce, R. J.; Romier, C.; Jung, M. Fluorescence-based screening assays for the NAD^+-dependent histone deacetylase smSirt2 from Schistosoma mansoni. **2014**.
Journal of Biomolecular Screening, Impact Factor: 2.207.

VIII. Ntie-Kang, F.; Nwodo, J. N.; Ibezim, A.; Simoben, C. V.; **Karaman, B**.; Ngwa, V. F.; Sippl, W.; Adikwu, M. U.; Mbaze, L. M. a. Molecular Modeling of Potential Anticancer Agents from African Medicinal Plants. **2014**.
Journal of Chemical Information and Modeling, Impact Factor: 4.068.

IX. Akkurt, M.; Guzeldemirci, N. U.; **Karaman, B.**; Buyukgungor, O., 2-[6-(4-Chloro-phen-yl)imidazo[2,1-b][1,3]thia-zol-2-yl]-N'-[(E)-4-meth-oxy-benzy l-idene]acetohydrazide. **2010**.
Acta Crystallographica Section E-Structure Reports Online. Impact Factor: 0.41

Oral Communications

2014 Development and validation of MMGB(-8)SA model for predicting the biological activity of sirtuin inhibitors.
2nd International BAU Drug Design Congress, Istanbul. (INVITED)
28th Molecular Modeling Workshop, Erlangen. (CONTRIBUTED)

2013 3,5-Bisarylidene-pyrrolidine-2,4-diones as Novel Inhibitors of Sirtuins.
BAU-Drug Design Symposium, Istanbul. (INVITED)

2012 Docking and Binding Free Energy Calculations of Inhibitors of SIRT2.
6th Summerschool Medicinal Chemistry, Regensburg. (CONTRIBUTED)

Poster Presentations

2014 Development and validation of MMGB(-8)SA model for predicting the biological activity of sirtuin inhibitors. **Karaman, B.** and Sippl, W.
28th Molecular Modeling Workshop, Erlangen.

2013 3,5-Bisarylidene-pyrrolidine-2,4-diones as Novel Inhibitors of Sirtuins. **Karaman, B.;** Huber, K.; Schröder, C.; Schemis, J.; Poschenrieder, H.; Jung M.; Bracher, F. and Sippl, W.
Innovative Approaches to Computational Drug Discovery Workshop, Lausanne.
BAU-Drug Design Symposium, Istanbul.

2012 Docking and Binding Free Energy Calculations of Inhibitors of SIRT2. **Karaman, B.;** Rumpf, T.; Tarikogullari, A. H.; Akgul, O.; Jung, M. and Sippl, W.
6th Summerschool Medicinal Chemistry, Regensburg, 2012.

2010 New [6-(4-chlorophenyl)imidazo[2,1-b]thiazole]derivatives: Synthesis and Anticancer Activity. **Karaman, B.** and Ulusoy, G. N.
Third International Meeting On Pharmacy & Pharmaceutical Sciences (IMPPS-3), Istanbul.

Additional Skills

Computer Skills

- OS: Linux, Windows
- Cheminformatics software/server: MOE, GOLD, Schrödinger, ParaDocks, Amber, VMD, LigandScout, SWISS-MODEL, MODELLER, PROCHECK, OpenEye (incl. ROCS&EON), PyMol, Chimera, SciFinder, MarvinSketch, ACD/ChemSketch
- Basic bash scripting
- MS Office

Methodologies

- Docking
- Homology modeling
- Molecular dynamics simulation
- Binding free energy calculation
- QSAR model development
- Virtual screening (structure- and ligand-based, e.g. docking, substructure and similarity search, pharmacophore-based VS)

Languages

- English (excellent/fluent), German (intermediate), Turkish (native)

Hobbies

Painting, swimming, travelling, new softwares/technologies.